

**HYDRODYNAMIC INERTIAL MASS
TESTING OF ECCS SUCTION STRAINERS**

Test Report No. TR-ECCS-GEN-01-NP

9711050002 971024
PDR ADCK 05000237
PDR



DE&S
Duke Engineering & Services

DUKE ENGINEERING & SERVICES, INC.
COMPANY DISCLAIMER STATEMENT

Please Read Carefully

The purpose of this report is to document the results of a hydrodynamic test program conducted by Duke Engineering & Services (DE&S) to investigate the behavior of large capacity stacked disk Emergency Core Cooling System (ECCS) strainers subjected to accelerated separated fluid flow fields. DE&S makes no warranty or representation (expressed or implied) with the respect to this document, and assumes no liability as to the completeness, accuracy, or usefulness of the information contained herein, or that its use may not infringe privately owned rights: nor does DE&S assume any responsibility for liability or damage of any kind which may result from the use of any of the information contained in this report. This report is also an unpublished work protected by the copyright laws of the United States of America.

EXECUTIVE SUMMARY

This report presents the results of a hydrodynamic test program conducted by Duke Engineering & Services (DE&S) to investigate the behavior of large capacity stacked disk Emergency Core Cooling System (ECCS) strainers subjected to accelerated separated fluid flow fields. The purpose of the test program was to generate the data required to develop empirically based values for the coefficients of constant velocity drag, C_d , and hydrodynamic (inertial) mass, C_m . Test results were obtained by accelerating the test objects through still water and by submerged free vibration tests.

The experimental investigation was designed and managed for DE&S by Dr. David Williams of Digital Structures, Inc. (DSI) and performed at the Offshore Model Basin (OMB) in Escondido, California. The tests were performed using Performance Contracting, Inc. (PCI) Sure-Flow™ stacked disk strainer prototypes.

This report describes the test program, test instrumentation, data reduction, and presents the results of the PCI stacked disk strainer hydrodynamic tests. The significant conclusions drawn from the reduction of the data recorded during the tests are as follows:

- The hydrodynamic coefficient of drag C_d , as expected, is higher than that for an impervious smooth cylindrical body of same major dimensions. < Proprietary Information Removed >
- The resultant coefficient of inertial mass, C_m , is substantially lower than that for an impervious smooth cylindrical body of same major dimensions. < Proprietary Information Removed >

These conclusions are applicable in the lateral direction to stacked disk strainers which are similar to the PCI prototype designs tested. This report discusses in detail those parameters which significantly influence the conclusions and which must be evaluated to determine their applicability.

TABLE OF CONTENTS

	Page
LIST OF TABLES	vi
LIST OF FIGURES	vii
INDEX OF NOTATIONS AND VARIABLES	viii
1.0 INTRODUCTION	1
1.1 Background	1
1.2 Approach	1
1.3 Objective	2
1.4 Report Layout	2
2.0 SCOPE OF TEST PROGRAM	2
2.1 General Description of Experiments	2
2.2 Test Specimens	3
3.0 DESCRIPTION OF TEST EQUIPMENT	11
3.1 Test Facility	11
3.2 Test Equipment	11
3.3 Test Instrumentation	12
3.4 Data Acquisition	12
4.0 TEST PROCEDURE	27
4.1 Test Matrix	27
4.2 Sequence of Testing Operations	28
4.3 Measurement of Strainer Weight and Dimensional Properties	30
4.4 Transducer/Instrumentation Calibration	30
4.5 Test Data Collection	31
4.6 Test Data Analysis	31
4.7 Test Monitoring	32
5.0 RESULTS	42
5.1 Approach to Results Interpretation	42
5.2 Constant Velocity Towing (Drag Forces)	43
5.3 Accelerated Towing (Hydrodynamic Mass)	44
5.4 Free Vibrations	45

6.0	DISCUSSION OF RESULTS	61
6.1	Approach to Results Interpretation	61
6.2	Coefficients of Drag	61
6.3	Coefficients of Hydrodynamic Mass	61
6.4	Vortex Shedding	62
6.5	Free Vibrations	63
6.6	Perforations and Hydrodynamic Mass Coefficients	63
6.7	Application of Test Results	64
7.0	CONCLUSIONS	68
8.0	REFERENCES	69

APPENDIX A

LIST OF TEST INSTRUMENTATION	A-1
------------------------------------	-----

APPENDIX B

CALIBRATION DATA	B-1
B-1. Load Calibration	B-2
B-2. Calibration Data	B-13
B-3. Velocity and Acceleration Calibration Data	B-21

LIST OF TABLES

	Page
4.1 Matrix for 100 Series Tests	33
4.2 Matrix for 200 Series Tests	34
4.3 Matrix for 300 Series Tests	35
4.4 Matrix for 400 Series Tests	36
4.5 Matrix for 500 Series Tests	37
4.6 Predicted Drag Forces	38
4.7 Predicted Inertia Forces	39
5.1 Constant Velocity Towing Test Results, Strainer Drag Forces	47
5.2 Constant Velocity Towing Test Results, Reference Body Drag Forces	48
5.3 Initial Impulse Towing Test Results, Strainer Inertia Forces	49
5.4 Initial Impulse Towing Test Results, Reference Body Inertia Forces	50
5.5 Free Vibration Test Results	51
6.1 Geometric Parameters of Tested Strainers	65

LIST OF FIGURES

	Page
2.1 Photo of PCI Sure-Flow™ Strainer, Prototype No. Test-1	5
2.2 Photo of PCI Sure-Flow™ Strainer, Prototype No. 2	6
2.3 Outline of PCI Sure-Flow™ Strainer, Prototype No. Test-1	7
2.4 Outline of PCI Sure-Flow™ Strainer, Prototype No.2	8
2.5 Photo of Reference Smooth Test Cylinder	9
2.6 Photo of Reference Smooth Impervious Stacked Disk Strainer	10
3.1 Overview and Layout of the OMB Towing Basin	14
3.2 Photos of the OMB Basin and Towing Carriage	15
3.3A OMB Subframe Arrangement (Rear View)	16
3.3B OMB Subframe Arrangement (Side View)	17
3.4 Photo of OMB Load-Cells to Subframe Arrangement	18
3.5 Layout of OMB Load-Cell Measuring System on Subframe	19
3.6 Photo of DSI/OMB Subframe with Strainer Adapter	20
3.7 Layout of DSI/OMB Strainer Adapter	21
3.8 Layout of DSI/OMB Test Specimen Boundary/Flow Deflector	22
3.9 Photo of DSI/OMB Test Specimen Boundary/Flow Deflector	23
3.10 DSI/OMB Test Specimen Boundary/Flow Deflector with Strainer Adapter	24
3.11 Layout of Test Instrumentation	25
3.12 Block Diagram of Data Acquisition System	26
4.1 Example of Target Travel Definition	40
4.2 Layout of Load Calibration System	41
5.1 Velocity History - Test d105a	52
5.2 Prototype No. Test-1 Drag Force History - Test d104	53
5.3 Prototype No. Test-1 Velocity History - Test d104	54
5.4 Support Drag Force History - Test d203	55
5.5 Prototype No. Test-1 Derived Overturning Moment History - Test d187	56
5.6 Prototype No. Test-1 Effective Lever Arm - Test d187	57
5.7 Prototype No. Test-1 Free Vibration Acceleration - Test d198a	58
5.8 Prototype No. 2 Free Vibration Acceleration - Test d598	59
5.9 Prototype No. 2 Free Vibration Load Cell FZ1 Force - Test d598	60
6.1 Recommended Drag Coefficient Values	66
6.2 Smooth Impervious Strainer Drag Force - Test d472	67

INDEX OF NOTATIONS AND VARIABLES

A	projected area normal to flow (ft ²)
C	absolute damping (lb-s/in)
C _{cr}	critical damping (lb-s/in)
C _d	hydrodynamic standard (velocity) drag coefficient
C _m	hydrodynamic acceleration (inertial mass) drag coefficient
δ	logarithmic decrement
dU/dt	acceleration (ft/s ²)
F _d	hydrodynamic standard drag (velocity) force component (lbs)
F _h	total hydrodynamic force (lbs)
F _i	impulse force (lbs)
F _m	hydrodynamic acceleration (inertial) drag forces component (lbs)
f	frequency (Hz)
ρ	water mass density (=1.9366 lbf-s ² /ft ⁴)
U	velocity (ft/s)
V	displaced enclosed volume (ft ³)
W	strainer air weight (lbs)
W _i	inertial mass weight (lbs)
W _s	weight of support assembly from the adapter up to and including horizontal load cells (lbs)
w	undamped natural frequency (Hz)
w _d	damped natural frequency (Hz)
X	peak amplitude of response

1.0 INTRODUCTION

1.1 Background

The installation and use of large-capacity passive suction strainers is a planned modification to allow BWR operators to comply with the new USNRC requirements for Emergency Core Cooling System (ECCS) (Reference 1.1). The subsequent analysis for qualification of the new installation requires calculation of hydrodynamic loading typical for submerged structures in a BWR suppression pool.

The hydrodynamic mass for the structural analyses is currently based on an inertial mass coefficient, C_m , of 2.0 (added mass coefficient of 1.0). No empirical data has been used to develop or substantiate this value, consequently the default value of 2.0 is being used. In view of the perforated nature of the strainer, and the end effect for bolt-on stacked disk strainers, it is believed that this is a conservative value. Literature surveys have not revealed any empirically-derived values for C_m that would be relevant to the strainers in this or any other application.

On this basis it was believed that the most pragmatic approach to substantiating a C_m value for use in structural qualification analyses was by undertaking a relatively simple hydrodynamically-based experimental derivation of C_m for one or more prototypical stacked disk bolt-on strainers.

The subject test program was undertaken by Duke Engineering & Services, Inc. (DE&S). The experimental investigation was designed and managed by Digital Structures, Inc. (DSI) and performed at the Offshore Model Basin (OMB).

1.2 Approach

The subject test program was designed to obtain a C_m value by application of basic fluid mechanics related to the forces on a cylinder due to fluid flow. The empirically-based Morison equation for separated flow around cylinders has provided a useful and somewhat heuristic approximation (Reference 1.2). The forces consist of a drag component and an inertial component. The drag component is proportional to the square of the fluid velocity (relative to a fixed cylinder) whereas the inertial component is proportional to the fluid acceleration. Changing the frame of reference, the same force components exist when the cylinder is accelerated through still water (i.e. the relative motion between the fluid and cylinder are maintained).

By measurement of the total forces to accelerate a body through fluid and a separate measurement of the drag forces and body acceleration, the hydrodynamic inertial forces can be derived and thus an effective mass coefficient C_m can be determined.

1.3 Objective

The purpose of the test program was to generate the data required to develop an empirically-based value for the hydrodynamic inertial mass coefficient, C_m , for use in qualification calculations related to installation of replacement ECCS suction strainers in BWR suppression pools. Other related hydrodynamic properties were also determined.

Lateral hydrodynamic loads (flow normal to the axis of the strainer) are the major concern and were the focus of this test program. Structural loads imparted on the strainers due to axially-directed flow (along the strainer axis) are typically of much smaller magnitudes and may therefore be estimated using classical hydrodynamic formulations. Hence, flow oriented along the strainer axis was not addressed in this test program.

1.4 Report Layout

The scope of investigation including a description of test specimens is summarized in Section 2. The facility and test equipment are described in Section 3 and Section 4 provides an outline of the test procedure. The test results are presented in Section 5 and discussed in Section 6. Findings and conclusions from the tests are summarized in Section 7. References are provided in Section 8 and Appendices A and B contain test instrumentation descriptions and calibration data, respectively.

2.0 SCOPE OF TEST PROGRAM

2.1 General Description of Experiments

The test program consisted of hydrodynamic experiments on two typical ECCS bolt-on stacked disk strainers. The test strainer was towed through nominally still water, with the strainer axis oriented normal to the travel direction. Various kinematic conditions were investigated. A reference cylinder and a reference

non-perforated stacked disk assembly were also tested for comparative purposes.

Several nominally-constant velocity conditions were attained to determine drag effects and obtain appropriate values for drag coefficient, C_d . Thereafter, testing under accelerated motions (simulating accelerated flow effects) was performed. Free vibration tests (quick-release "pluck" tests) of all the specimens in the submerged condition were also undertaken.

Subsequently, the hydrodynamic inertial effects on the test strainer were derived, from which an effective nominal coefficient of hydrodynamic mass, C_m , was calculated.

2.2 Test Specimens

The two strainer test specimens for this program consisted of the Performance Contracting, Inc., BWR stacked disk test strainers (PCI Sure-Flow Strainer, Prototype No. Test-1 and Prototype No. 2). The former is a relatively small 6-disk strainer (65 ft²) for nominal 10-inch pipe, whereas the latter is a large 13-disk strainer (170 ft²) for 24-inch pipe, detailed respectively in the PCI shop drawings, References 2.1 and 2.2, and shown in Figures 2.1 and 2.2. The disks were made from 11 gauge perforated plate with 1/8 inch diameter holes and 40 percent open area.

The outside diameters of the disks for the small and large strainers are 30 and 40 inches, respectively. As indicated in Figures 2.3 and 2.4, the overall lengths shown are respectively 33 and 54 inches. The significant dimensions were verified at the test site. The only discrepancy was that for the large strainer the spool length was 5-1/2 inches, not 6 inches, giving an overall length of 53-1/2 inches. The projected net lateral frontal area of the small and large strainer was respectively 5.28 and 12.0 ft² (gross areas of 6.48 and 14.33 ft²).

The test strainers were also weighed at the test site. The air weights were 305 and 948 lbs respectively for the small and large strainer (including the internal suction flow control device). Enclosed volumes were 9.04 and 26.27 ft³ (12.40 and 36.35 ft³ gross). The associated water displacements were 564 and 1638 lb (777 and 2267 lb gross).

A Reference Smooth Test Cylinder was fabricated by wrapping the small strainer with 33 inch wide, 18 gauge (0.048 inch) aluminum sheet metal. The sheet metal was secured to the outer diameter of the strainer with self-drilling sheet metal screws. The cylinder free end was covered with a 1/8 inch thick circular

plastic board and secured to the perforated strainer using the same kind of self-drilling sheet metal screws (shown in Figure 2.5). The resulting cylinder was 33 inches long and of uniform 30 inches diameter (up to the flange). The cylinder weighed 324 lb in air and had a total surface area (including free end) of 26.5 ft². Because the wrapping extended up to the flange, the total projected lateral area, 6.875 ft², of the Reference Test Cylinder was slightly larger than that for the gross enveloped projected area of the Small PCI Strainer No. Test-1 (6.48 ft²).

The purpose of the Reference Cylinder Test was to provide a basis for comparisons with the perforated strainer and standard cylindrical shapes, with end effects.

A Reference Smooth Impervious Stacked Disk Assembly was created by wrapping the small perforated PCI Strainer Prototype No. Test-1 with self-adhesive clear plastic sheets (contact paper) and duct tape to fully cover the entire strainer, as shown in Figure 2.6. Several 1/8 inch holes were punched through the plastic at the free end to allow flooding. The air weight was 308 lb and the total surface area, including spool was 66 ft². The projected net lateral area was 5.28 ft² (gross "envelope" area of 6.48 ft² to outside profile).

The purpose of this test specimen was to provide a direct comparison with the perforated stacked disk strainer.

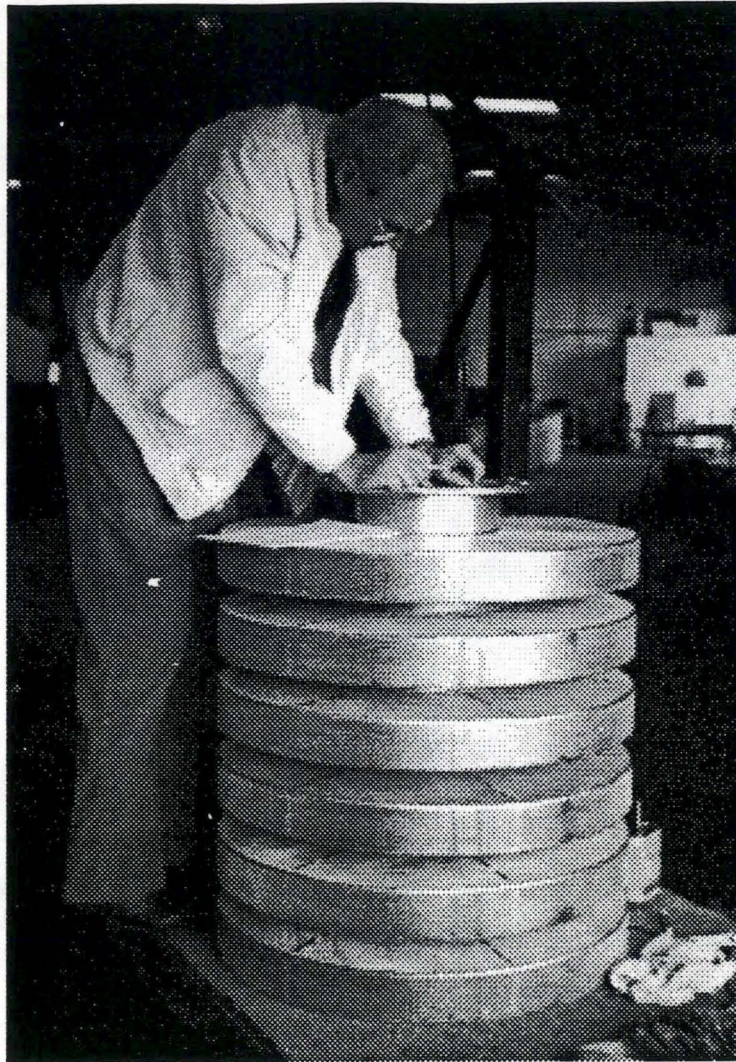


FIGURE 2.1

PCI SURE-FLOW™ STRAINER PROTOTYPE NO. TEST-1

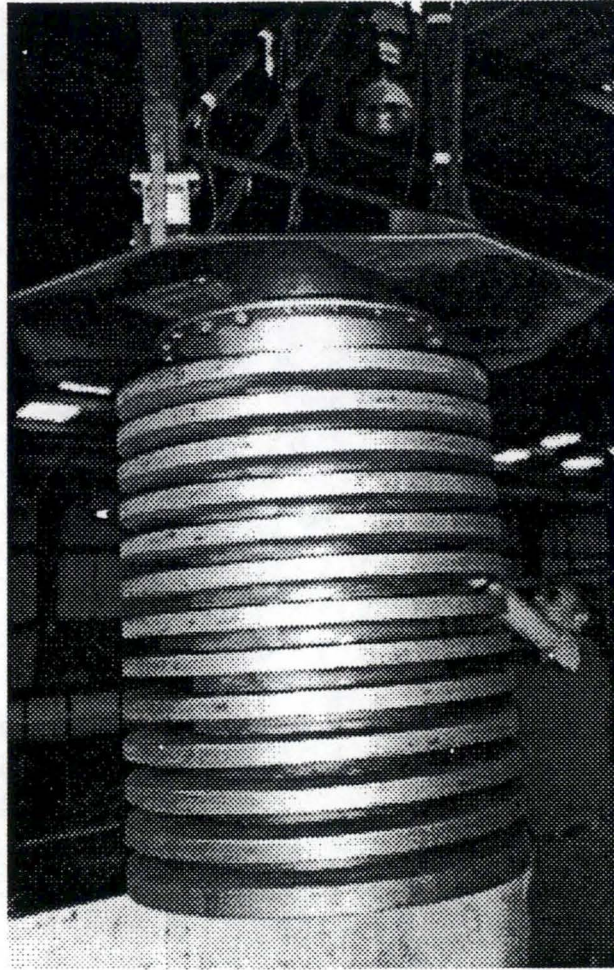


FIGURE 2.2

PCI SURE-FLOW™ STRAINER PROTOTYPE NO. 2

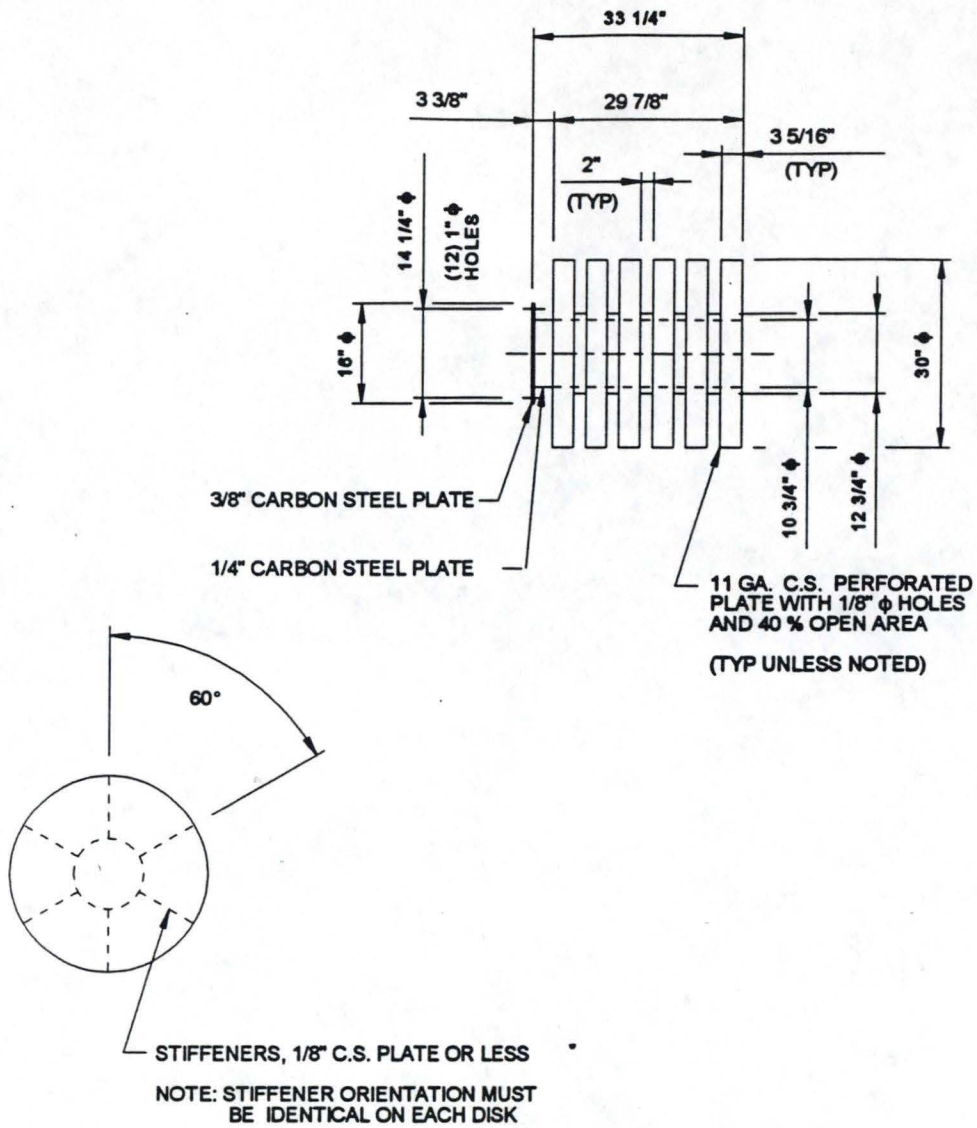


FIGURE 2.3

PCI SURE-FLOW™ STRAINER PROTOTYPE NO. TEST-1

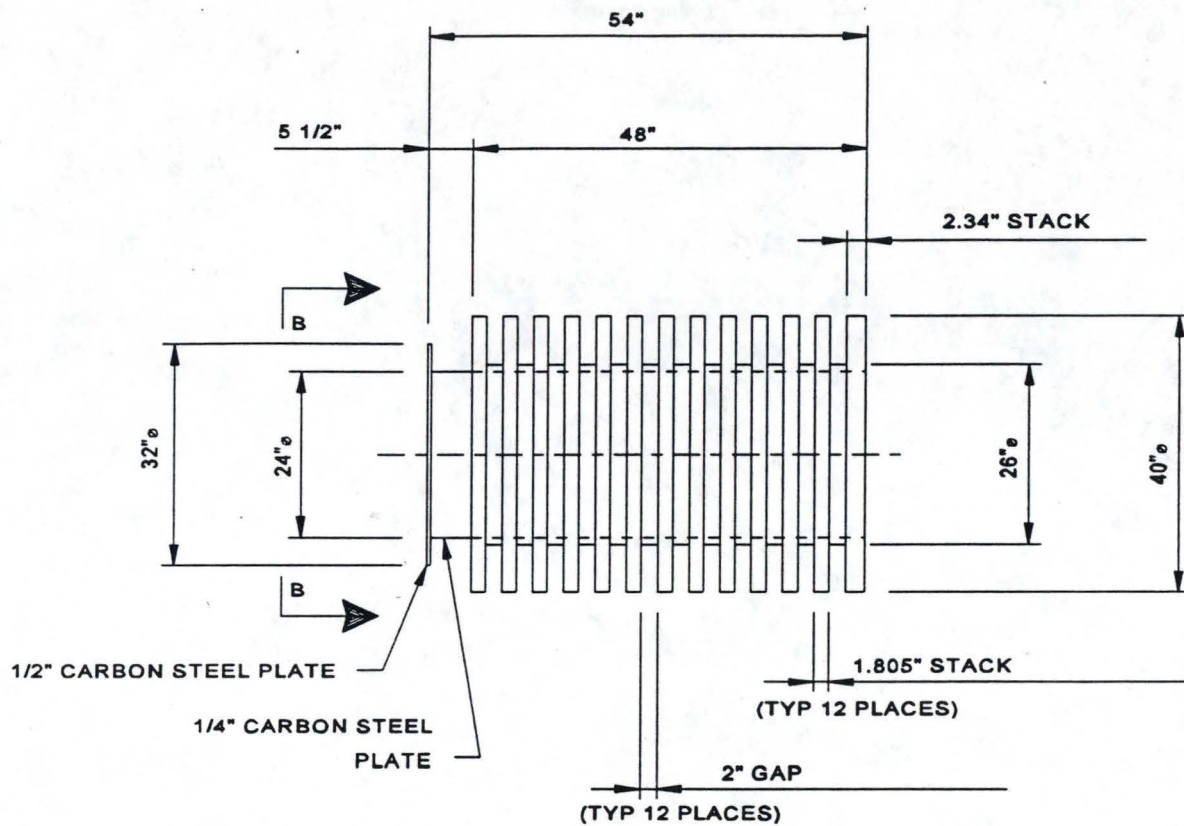


FIGURE 2.4

OUTLINE OF PCI SURE-FLOW™ STRAINER PROTOTYPE NO. 2



FIGURE 2.5

REFERENCE SMOOTH TEST CYLINDER



FIGURE 2.6

REFERENCE SMOOTH IMPERVIOUS STACKED DISK STRAINER

3.0 DESCRIPTION OF TEST EQUIPMENT

3.1 Test Facility

The tests were performed in accordance with the test specification (Reference 3.1) at Offshore Model Basin's (OMB) Towing/Seakeeping Basin located at their facility in Escondido, California. The basin is 295 ft (90m) long, 48 ft (14.6m) wide and 15 ft (4.6m) deep. An overview and layout of the basin is shown in Figure 3.1.

3.2 Test Equipment

The OMB Towing Carriage, powered by two 30 HP DC electric motors, spans the basin and rides on rails (see Figure 3.2). Depending on the drag load, the Towing Carriage provides towing speeds ranging from 0.05 ft/sec to 18 ft/sec with computerized speed control and was used to tow the submerged test specimen through the basin.

The OMB Subframe, Figure 3.3, was attached to the towing carriage, so as to provide three-point support of the test specimen in the submerged arrangement. The load-measuring devices were attached to each of the three legs of the subframe as indicated in Figure 3.4 and 3.5. The Subframe weighed 152.9 lbs bare, and 205.7 lbs with the six (6) load cells and their mountings.

The DSI/OMB Strainer Adapter is a stiff three-legged Y-shaped fixture for transferring load from either strainer flange to the ball joints of the load cells on the subframe (see Figure 3.6 and 3.7). The strainer was bolted to the adapter with two bolts per leg, six bolts in all (7/8 inch and 1-1/4 inch diameter bolts, respectively, for the small and large strainer). The adapter, as used (with zinc anodes), weighed 179.3 lbs.

The DSI/OMB Test Specimen Boundary/Flow Deflector, (B/FD) an octagonal horizontal steel plate (3/8 inch thick, 60 inch dimension across flats) surrounding the adapter (Figure 3.8), was designed to prevent (or suppress) surface waves. It was connected to the subframe, above the load cell location, with three braces as shown in Figures 3.9 and 3.10. A small gap (approximately 1/2 inch) separated the B/FD from the adapter as shown in Figure 3.11. A 5 inch high bulwark on the forward edge was designed to minimize flow around the adapter (extraneous drag load). The load cells only measured extraneous flow loads from the adapter, not the boundary/subframe assembly. The B/FD weighed 269.1 lbs.

3.3 Test Instrumentation

The primary instrumentation consisted of the following transducers, detailed in Appendix A, and located as shown in Figure 3.11:

- Six independent strain-gaged load cells (I-beams) to measure the force history applied to the test specimen for the duration of each test. Three of these, FX1, FX2, FX3, measure longitudinal shear and were summed to provide the total horizontal applied force, X-Force. The other three, FZ1, FZ2, FZ3, measure vertical loads and were used to determine the overturning moment applied to the test specimen during the test. Each load cell was custom-built from a 4 inch cube aluminum block and waterproofed for submerged operation.
- An independent acceleration transducer (accelerometer), ACCX2S, mounted on the adapter above the test specimen flange, was provided to measure test kinematics and verify local test specimen motion and compare with the programmed motion of the towing carriage. Support flexibility effects could thus be taken into account. The adapter accelerometer was waterproofed for submerged operation.
- The carriage velocity was measured by the tachometer located near a carriage wheel.

Secondary instrumentation consisted of stop watch and standard measuring devices (tapes, calipers, etc).

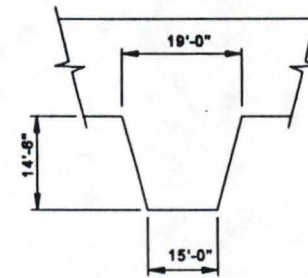
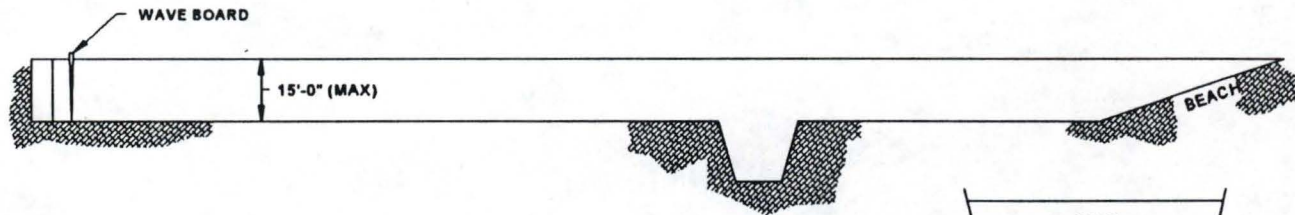
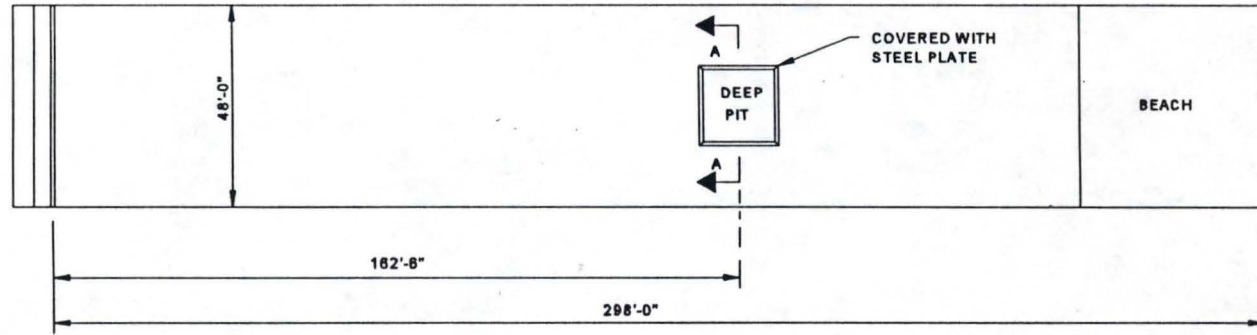
3.4 Data Acquisition

A block diagram of the data acquisition system used for this test program is shown in Figure 3.12. All transducers used provided analog signals. The analog input section includes an input multiplexer. Signal scaling is provided by a high-performance, differential input, programmable gain amplifier (PGA). The 12-bit A/D converter can be configured for different input voltage ranges to ± 10 volts full scale.

A hardware channel scanner enhances high-speed and DMA (Direct Memory Access) performance. Essentially, the A/D Converter Board writes analog transducer voltage data directly to disk via an internal timer when operating in the DMA mode.

The PC applications package 386-MATLAB (Reference 3.2) was used to convert all data to engineering units and to perform other basic data processing. The output from this processing includes data files that were plotted.

Note that the calibration procedure was end-to-end (transducer input to processed digital output) to eliminate the need to calibrate any and all parts of the process and thus simplify quality assurance (QA) of the data collection.



SECTION A-A

FIGURE 3.1

OVERVIEW AND LAYOUT OF THE OMB TOWING BASIN

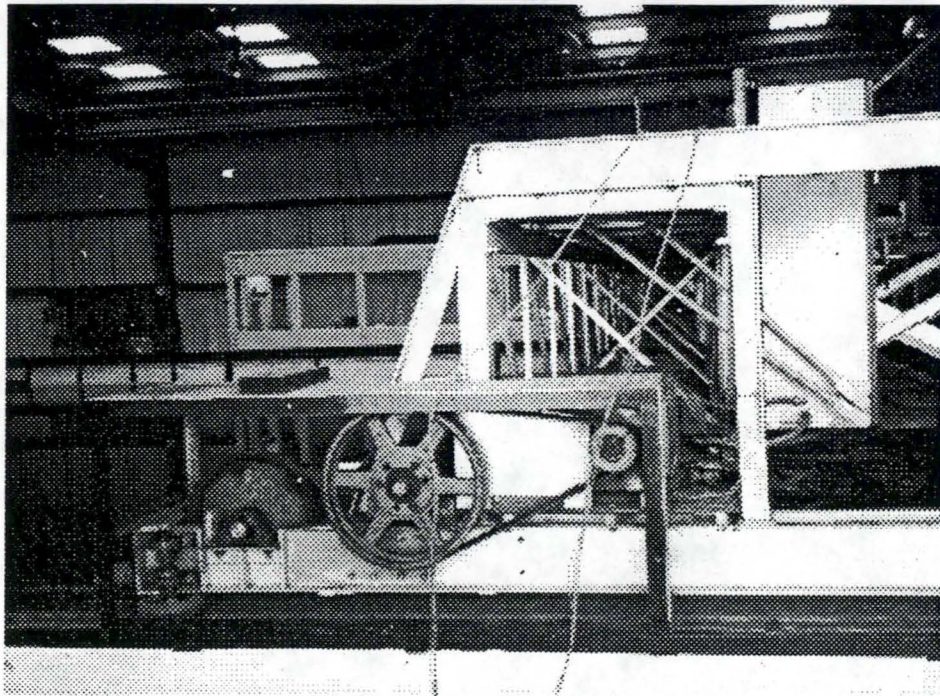
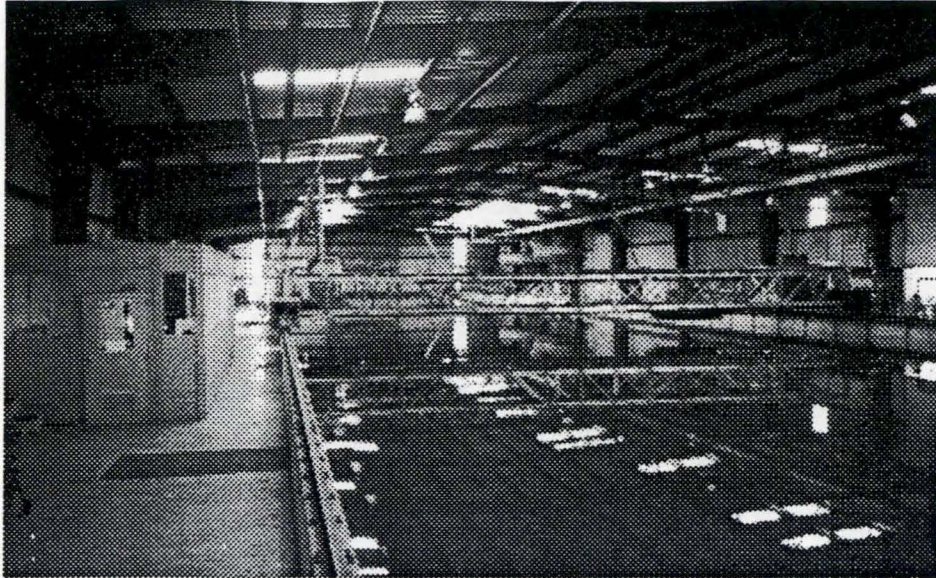


FIGURE 3.2

OMB BASIN AND TOWING CARRIAGE

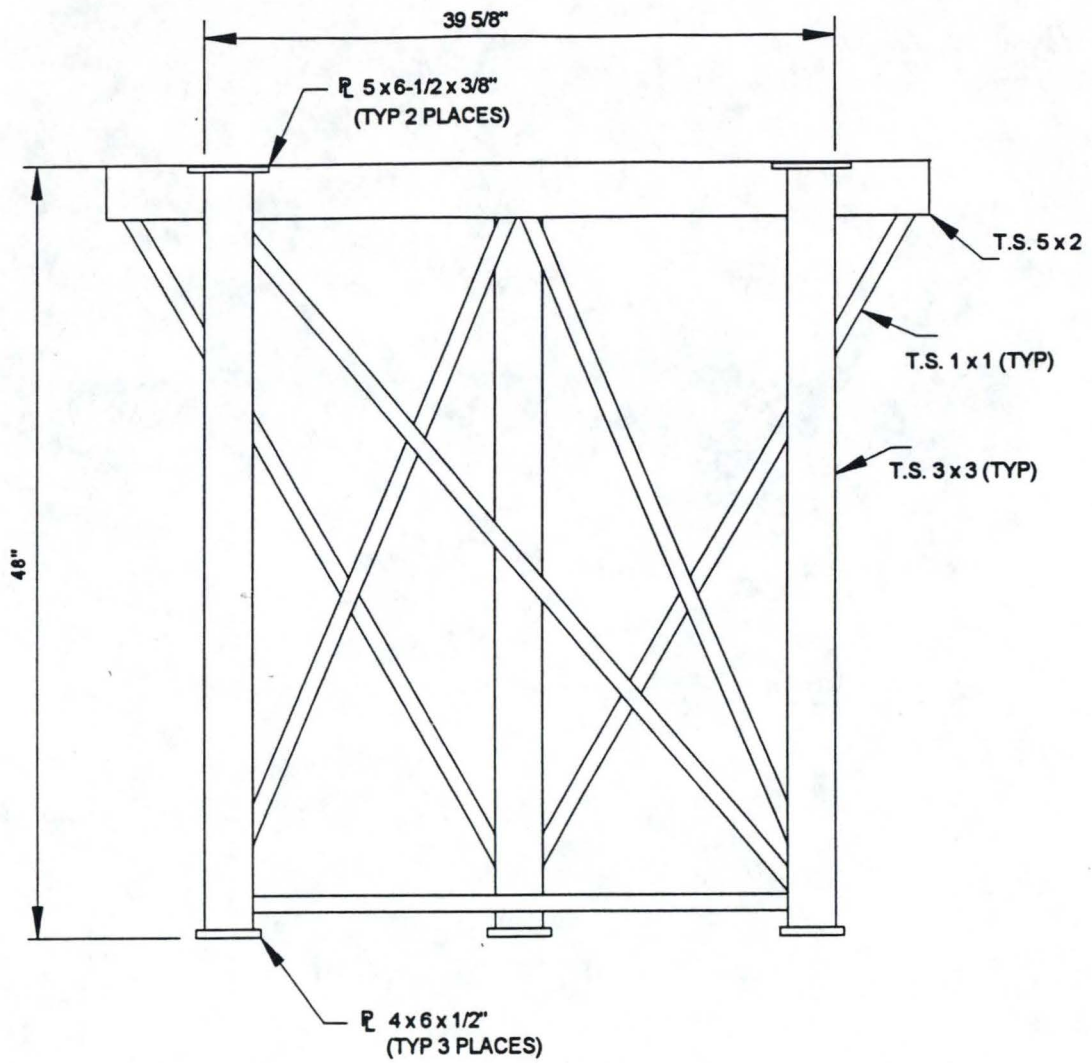


FIGURE 3.3A

OMB SUBFRAME ARRANGEMENT (REAR VIEW)

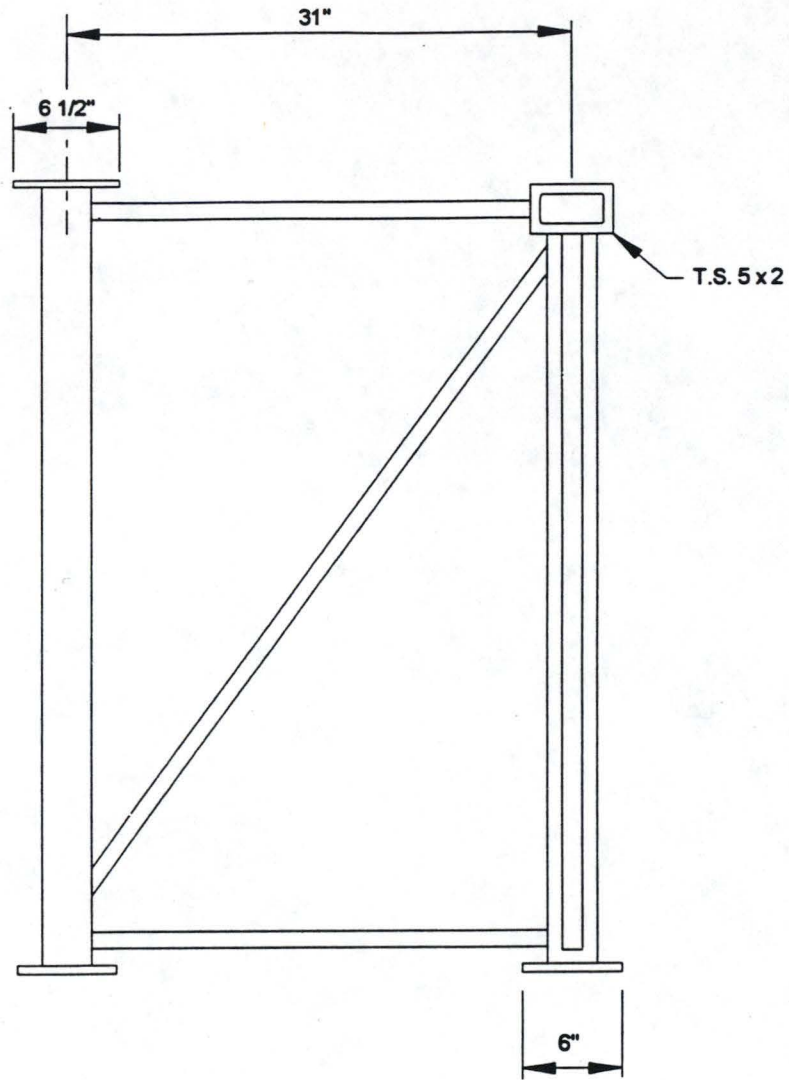


FIGURE 3.3B

OMB SUBFRAME ARRANGEMENT (SIDE VIEW)

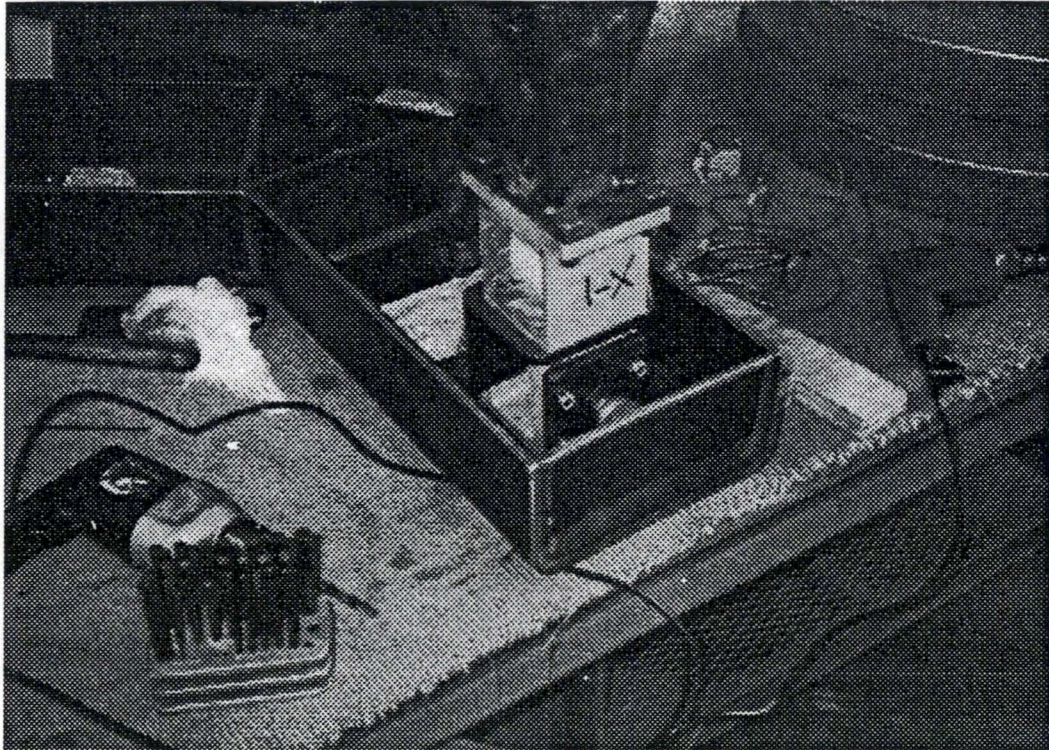


FIGURE 3.4

OMB LOAD CELLS TO SUBFRAME ARRANGEMENT

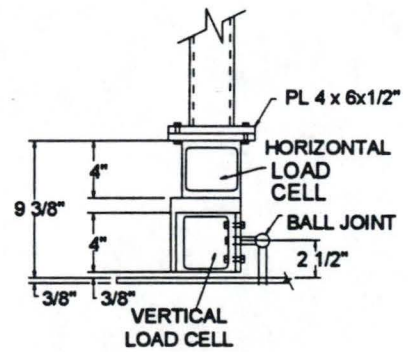
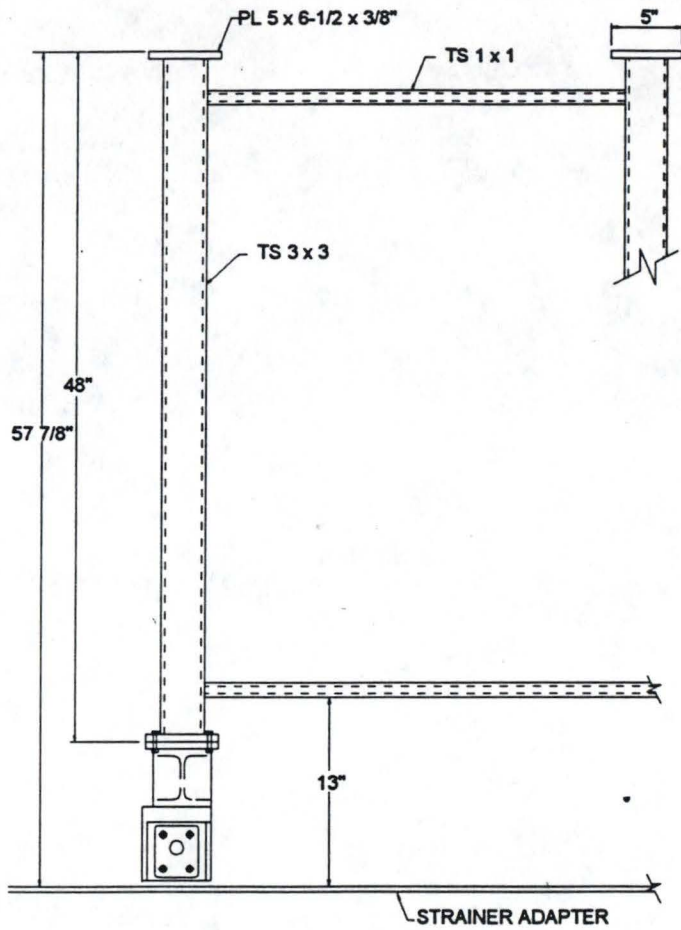


FIGURE 3.5

OMB LOAD CELL MEASURING SYSTEM ON SUBFRAME

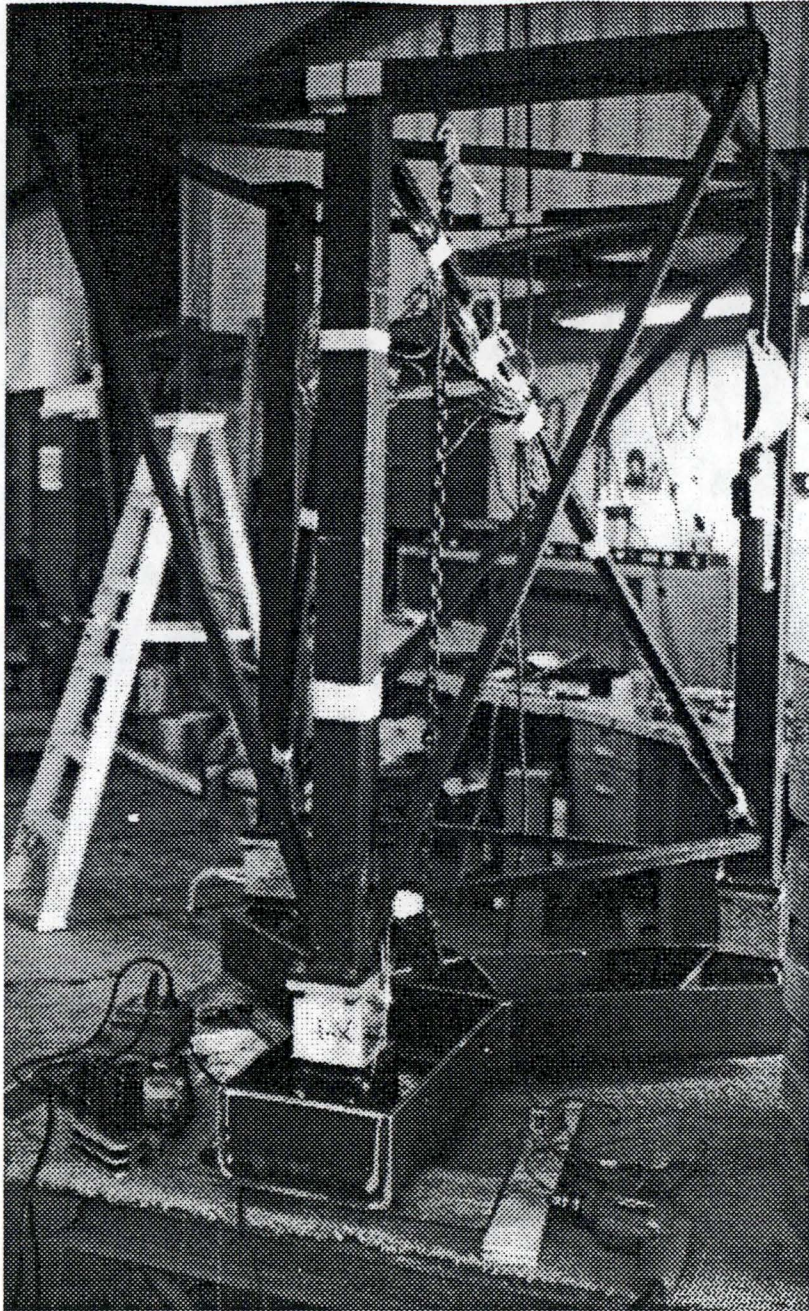


FIGURE 3.6

DSI/OMB SUBFRAME WITH STRAINER ADAPTER

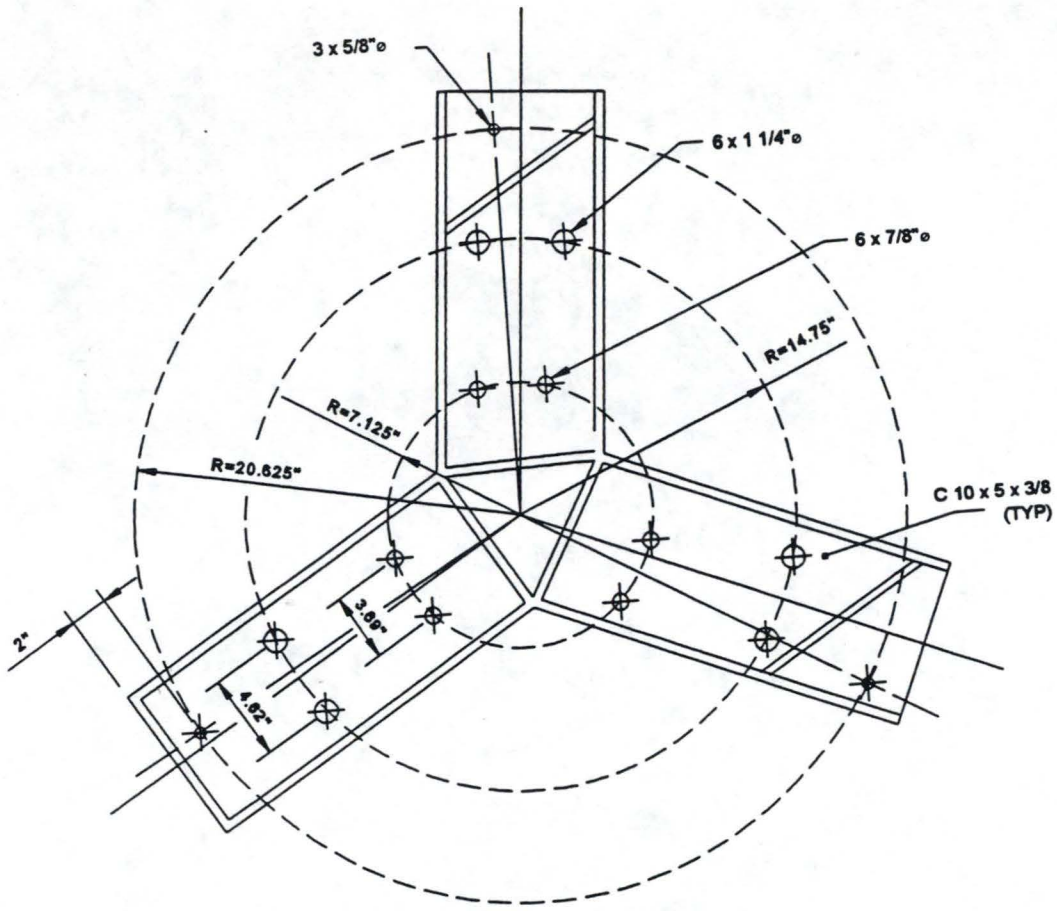
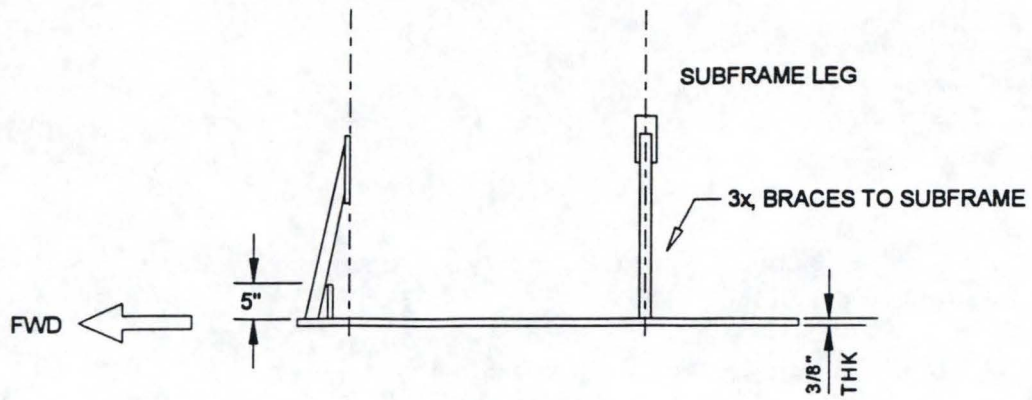


FIGURE 3.7
LAYOUT OF DSI/OMB STRAINER ADAPTER



SECTION A-A

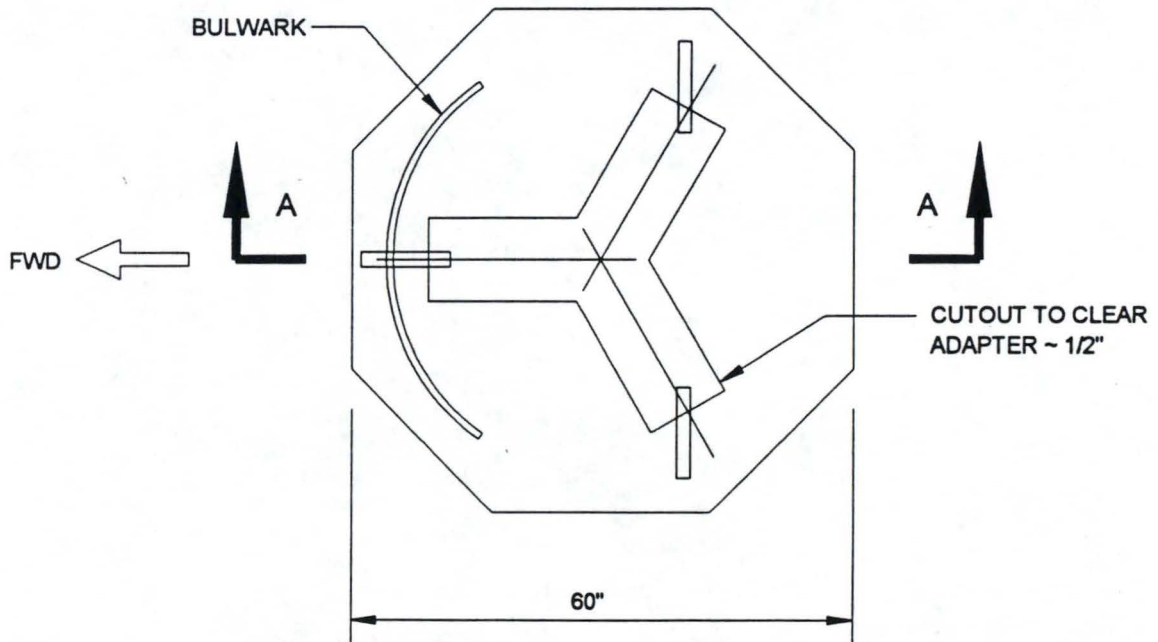


FIGURE 3.8

LAYOUT OF DSI/OMB TEST SPECIMEN BOUNDARY/FLOW DEFLECTOR

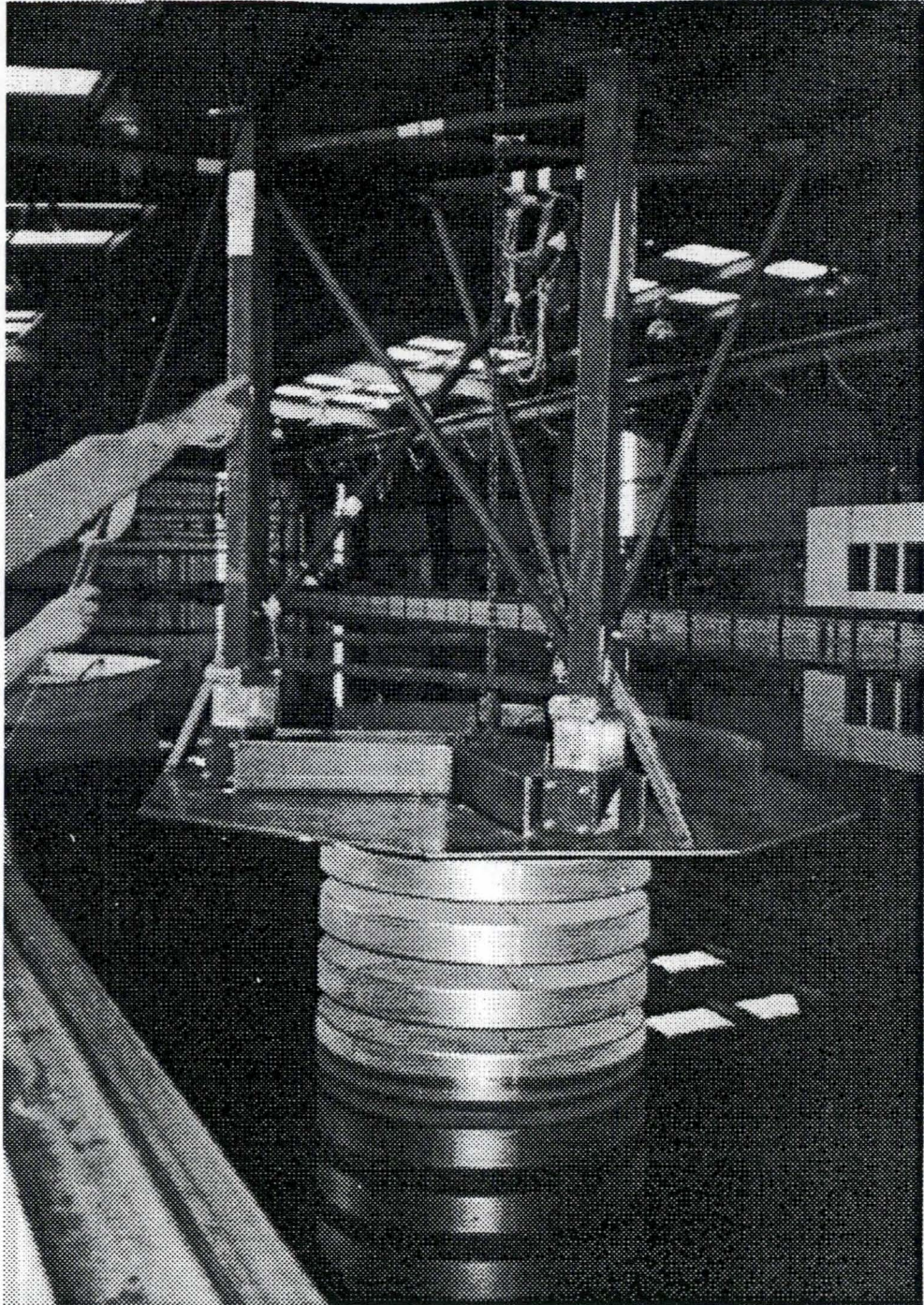


FIGURE 3.9

DSI/OMB TEST SPECIMEN BOUNDARY/FLOW DEFLECTOR

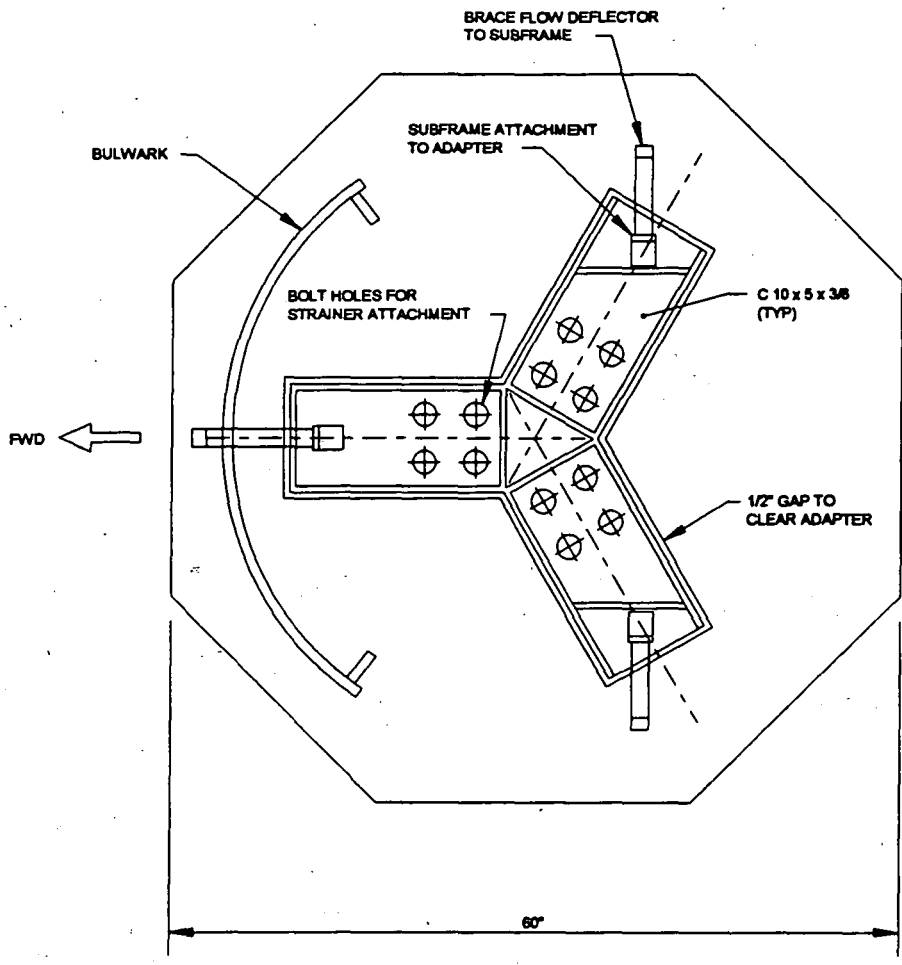


FIGURE 3.10

DSI/OMB TEST SPECIMEN BOUNDARY/FLOW DEFLECTOR WITH STRAINER ADAPTER

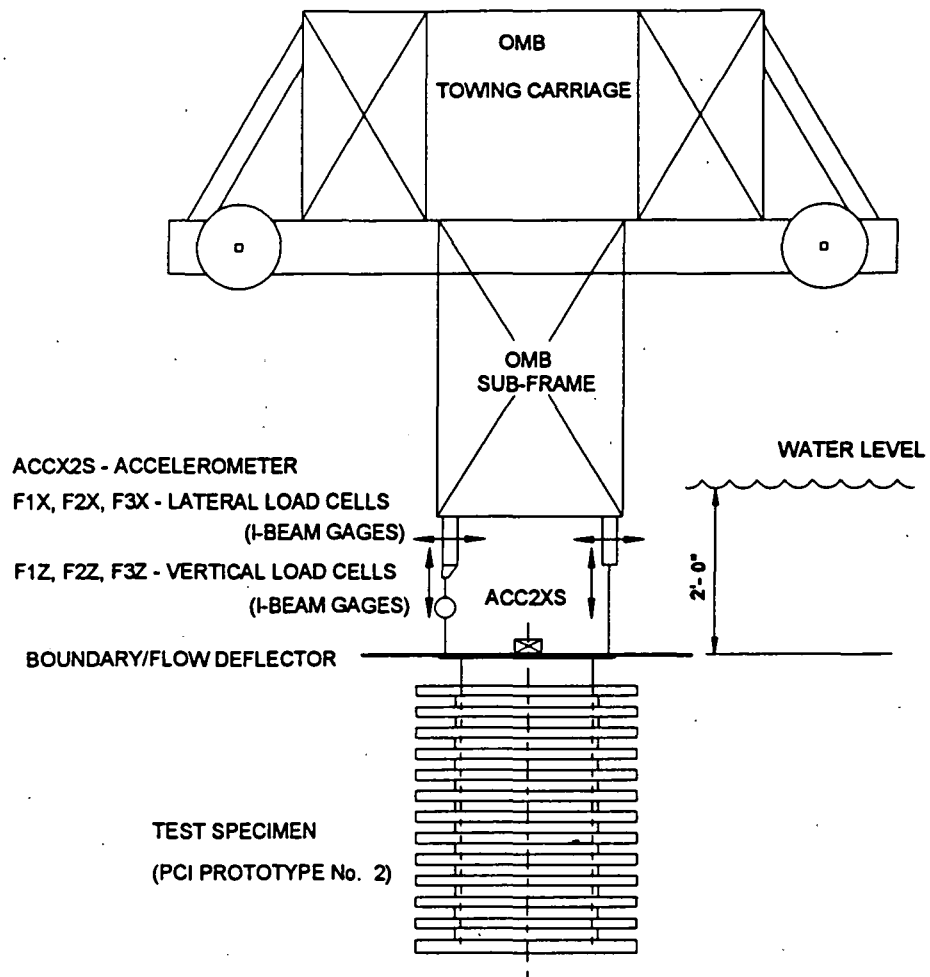


FIGURE 3.11

LAYOUT OF OMB LOAD-CELL MEASURING SYSTEM ON SUBFRAME

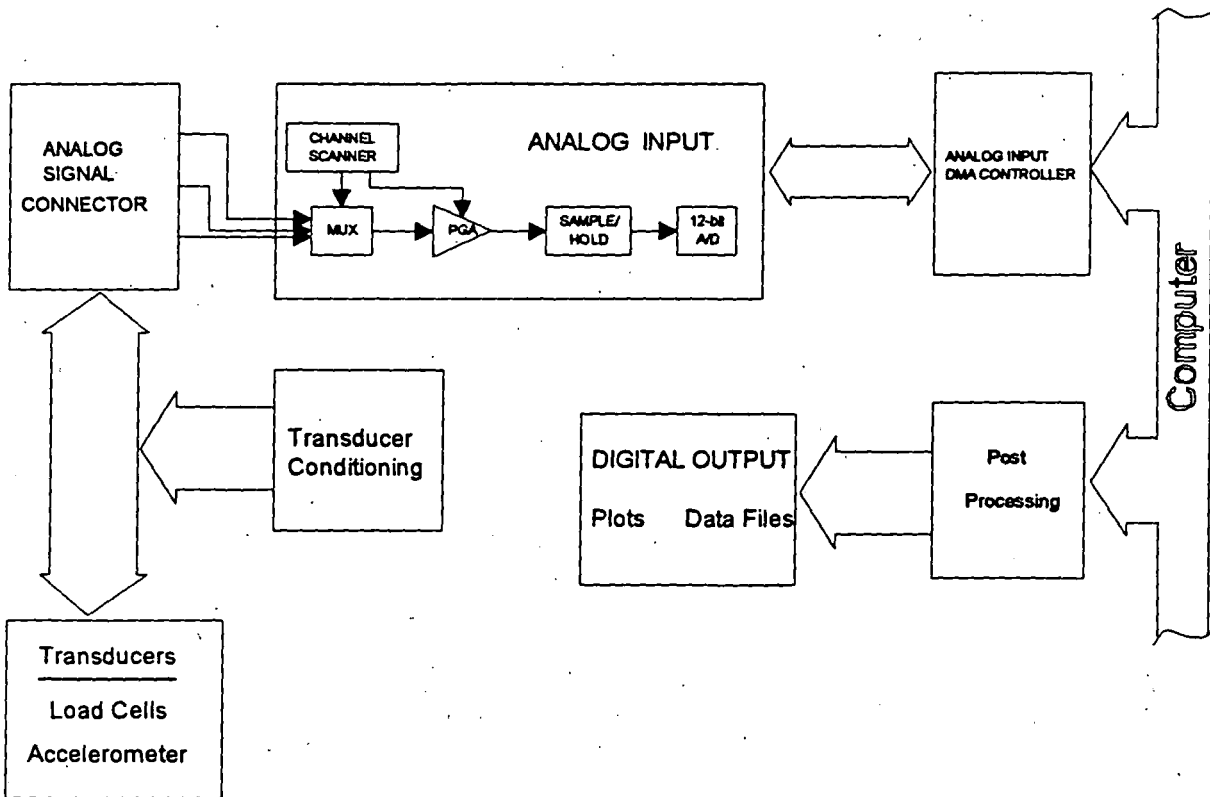


FIGURE 3.12

BLOCK DIAGRAM OF DATA ACQUISITION SYSTEM

4.0 TEST PROCEDURE

4.1 Test Matrix

Separate series of tests were undertaken for the small Prototype No. Test-1 Strainer (100 Series) and the large Prototype No. 2 Strainer (500 Series). In addition, tests were performed for; the adapter/boundary assembly alone (i.e. without a test specimen attached) (200 Series); the reference smooth test cylinder (300 Series); and the reference smooth impervious stacked disk (400 Series).

The tests conducted are indicated in Tables 4.1 through 4.5. The final test selection was dependent on the outcome of prior tests and was determined during conduct of the tests. The order of the tests in general followed the Test Number sequence shown in the Tables 4.1 through 4.5. The calibration checks are also indicated.

The initial tests for each series consisted of a slow build-up (approx. $\frac{1}{2}$ ft/s²) to a relatively constant velocity (nominally zero acceleration) as shown in the example target travel history of Figure 4.1, with the aim of establishing the drag coefficient for the test specimen. The sequence began with low terminal velocities of 2 ft/s, building to the high velocity of 10 ft/s in increments of 2 ft/s, so that velocity dependence of C_d could be investigated. Several tests were repeated.

The later tests for each series were at increasing accelerated flow to a prescribed terminal velocity, with the aim of generating hydrodynamic inertial forces so that the mass coefficient for the test specimen could be derived. The target accelerations ranged from a low value of 0.5 ft/s² to the high value of 3 ft/s². (This proved to be the limit for controlled motion of the towing carriage and in some cases, with large drag, was beyond the limit). The accelerated and decelerated stages had the same nominal absolute value.

An attempt was made to attain higher accelerations for short duration travel but control of the towing carriage was unstable and concern for equipment safety precluded higher accelerations being attained for the test specimens. In several cases the target accelerations could not be attained.

Repeated free vibration (pluck) tests of each specimen in the as-installed submerged condition were also undertaken and provided very consistent data.

Several towing tests were also repeated, based on either the desire to determine repeatability, to obtain more data for a particular situation, or in the case of

suspected equipment malfunction.

4.2 Sequence of Testing Operations

Each test series consisted of several separate stages:

(a) Presetting and Verification of Planned Test Travel

The following sequence of operations occurred during travel setting, undertaken before the first series of tests:

- Programming the planned test motion sequence (travel) in the controller for the towing carriage. The planned distance for each test was 200 ft.
- Running the towing carriage through the programmed travel and recording motions via the data acquisition system.
- Recording independent motion measurements of the carriage (distance and time, using tape measure and stop watch).
- Comparing independent and instrumentation-acquired motion measurements.
- Reconciling any differences.

(b) Test Specimen/Load-Measuring System Installation

The following sequence of operations occurred during test specimen installation:

- Mounting the instrumentation (load and acceleration transducers), Adapter and Boundary/Flow Deflector to the Subframe.
- Checking load cell preload and minimizing initial strain by shimming supports at bolt locations
- Mounting test specimen to the subframe assembly.
- Mounting the subframe with attached test specimen and

instrumentation to the towing carriage. The assembly was lifted into the basin and floated with ancillary buoyancy during the installation.

- Calibrating all instrumentation (per procedure below) in the as-installed condition.

(c) Towing Testing/Data Acquisition

The following operations occurred during each towing test:

- Beginning with the first test in series, all data (load on strainer and strainer acceleration and velocity) was recorded by the data acquisition system during conduct of the test. The standard data acquisition rate for towing tests was 8 samples per second for each channel.
- Following each test, the data was processed and plotted as a history of the appropriate response versus time for the test duration.
- After each test the towing carriage was returned to its original position at a slow speed to minimize wave generation.
- Preliminary checking of the test data was undertaken to determine if recalibration was required.

Subsequent tests followed the same general procedure.

(d) Free Vibration Testing/Data Acquisition

The following operations occurred during each free vibration test:

- A load of approximately 200 lbs was applied to the test specimen using the hanging weight load calibration system shown in Figure 4.2.
- The load was quick-released by cutting the line and the test specimen underwent submerged free oscillation.
- Response data (load on specimen and acceleration) was recorded

- Response data (load on specimen and acceleration) was recorded by the data acquisition system during the test. The standard data acquisition rate for free vibration tests was 50 samples per second for each channel.
- Following each test, the data was processed and plotted as a history of the appropriate response for the test duration.
- The free vibration tests were repeated three (or four) times.

4.3 Measurement of Strainer Weight and Dimensional Properties

The test strainers were weighed and the center of gravity determined by measurement (by balancing, single-point suspension and two-point weighing). The significant geometric dimensions, as indicated in the outlines of Figures 2.3 and 2.4, were checked and significant discrepancies noted as indicated in Section 2.2.

4.4 Transducer/Instrumentation Calibration

All transducers were calibrated and checked prior to testing and as shown in Tables 4.1 through 4.5. The complete calibration data is provided in Appendix B.

The calibration procedure was an end-to-end process (input to output) to eliminate the need to calibrate any and all parts of the process and thus simplify QA of the data collection.

Load calibration checking consisted of applying an independently measured force to the test specimen in the as-installed arrangement. The loads were applied in 100 lb increments to cover the range from no load to 500 lbs. The load was applied to the test specimen by a stout line attached to the specimen near the free end. The angle of the applied load to the horizontal (perpendicular to the strainer axis) was calculated from geometric measurements to the anchor. In all cases the angle was sufficiently small so that the horizontal component of the force was approximately equal to the applied force. The applied load was measured using a reference load indicator (proving ring), which in turn was calibrated using weights traceable to National Standards (NIST). The load cell output, after conditioning and undergoing data acquisition was recorded as a data file and plotted.

The recorded data values and plotted output were compared and reconciled with the applied load. No discrepancies (within reasonable tolerances of $\pm 2\%$) were evident throughout the test program.

Motion calibration consisted of acceleration and velocity measurements of the towing carriage. Distance and timing measurements were used to verify the nominally constant-velocity and uniform-acceleration motions.

Acceleration due to gravity was used as the reference for acceleration calibration (rotating the accelerometer through 180 degrees from upward orientation to downward orientation corresponds to a change in acceleration of 2g, from +g to -g). Smaller rotations (up to 15 degrees) were used to calibrate to low accelerations. The rotations were applied by means of an angle computer.

4.5 Test Data Collection

Each test run was labeled with a unique number for test results data identification purposes as indicated in Tables 4.1 through 4.5. The measured data for each test run was recorded by the data acquisition system and reviewed immediately after the test.

4.6 Test Data Analysis

Preliminary analysis of the acquired data consisted of plotting all measured responses as a function of time, and checking against independent measurements of parameters (e.g. time and distance) where possible.

For guidance, values of drag forces, F_d , at different velocities, U , with assumptions of 0.6 and 1.0 for the drag coefficient, C_d , based on projected area normal to flow, A , were calculated, as indicated in Table 4.6. All calculations were based on a water mass density, ρ , of 1.9366 lbf- s²/ft⁴ (20 C°). F_d was determined using the classical relationship (Reference 1.2):

$$F_d = \frac{1}{2} C_d \rho A U|U| \quad \text{Eq [1]}$$

Similarly, values of inertial forces, F_m , at accelerations, dU/dt , of 1.5 and 3.0 ft/s², with assumptions of 1.0, 1.5 and 2.0 for the inertial mass coefficient, C_m , based on displaced enclosed volume, V , were also calculated, as indicated in Table 4.7. The total weight is the specimen weight, W , plus the hydrodynamic

weight, $C_m \cdot \rho g V$ (contained and added mass). F_m was based on the widely accepted relationship:

$$F_m = C_m \rho V dU/dt \quad \text{Eq [2]}$$

4.7 Test Monitoring

All tests were monitored and witnessed by qualified test engineers.

TABLE 4.1

MATRIX FOR 100 SERIES TESTS

SMALL STACKED DISK BOLT-ON STRAINER PCI PROTOTYPE NO. TEST-1

Test Number	Target Velocity (ft/s)	Target Acceleration (ft/s ²)	Comments
d100			
d101	2	0.5	
d102	4	0.5	
d103	6	0.5	
d103a	6	0.5	
d103b	6	0.5	
d104	8	0.5	
d104a	8	0.5	
d105	10	0.5	
d105a	10	0.5	
d1051	6	1.0	
d1052	10	1.0	
d161	6	1.5	
d162	10	1.5	
d171	6	2.0	
d172	10	2.0	
d181	6	2.5	
d182	10	2.5	
d185	6	2.8	
d186	6	3.0	
d187	10	2.8	
d188	10	3.0	
d198			
d198a			
d198b			
d198c			
d197			

< Proprietary Information Removed >

TABLE 4.2

MATRIX FOR 200 SERIES TESTS

DSI/OMB STRAINER ADAPTER/BOUNDARY ASSEMBLY ALONE

Test Number	Target Velocity (ft/s)	Target Acceleration (ft/s ²)	Comments
d201	2	0.5	< Proprietary Information Removed >
d202	4	0.5	
d203	6	0.5	
d204	8	0.5	
d205	10	0.5	
d252	10	1.0	
d262	10	1.5	
d272	10	2.0	
d282	10	2.5	
d283	10	2.8	
d286	6	3.0	
d288	10	3.0	
d298			
d298a			
d298b			

TABLE 4.3

MATRIX FOR 300 SERIES TESTS

REFERENCE TEST CYLINDER WITH BOUNDARY - 30"φ X 33.25" LONG

Test Number	Target Velocity (ft/s)	Target Acceleration (ft/s ²)	Comments
d301	2	0.5	< Proprietary Information Removed >
d302	4	0.5	
d303	6	0.5	
d304	8	0.5	
d305	10	0.5	
d352	10	1.0	
d362	10	1.5	
d372	10	2.0	
d382	10	2.5	
d383	10	2.8	
d386	6	3.0	
d398			
d398a			
d398b			

TABLE 4.4

MATRIX FOR 400 SERIES TESTS

REFERENCE IMPERVIOUS STACKED DISK ASSEMBLY
COVERED PCI PROTOTYPE NO. TEST-1

Test Number	Target Velocity (ft/s)	Target Acceleration (ft/s ²)	Comments
d401	2	0.5	< Proprietary Information Removed >
d402	4	0.5	
d403	6	0.5	
d404	8	0.5	
d405	10	0.5	
d452	10	1.0	
d462	10	1.5	
d472	10	2.0	
d482	10	2.5	
d498			
d498a			
d498b			
d498c			
d499			

TABLE 4.5

MATRIX FOR 500 SERIES TESTS

LARGE STACKED DISK BOLT-ON STRAINER PCI PROTOTYPE NO. 2

Test Number	Target Velocity (ft/s)	Target Acceleration (ft/s ²)	Comments
d501	2	0.5	< Proprietary Information Removed >
d501a	2	0.5	
d502	4	0.5	
d503	6	0.5	
d504	8	0.5	
d505	8	0.5	
d505a	10	0.5	
d552	8	1.0	
d562	8	1.5	
d572	8	2.0	
d582	8	2.5	
d587	8	2.8	
d598			
d598a			
d598b			
d598c			
d599			
d599a			

TABLE 4.6

CALCULATED DRAG FORCES (lbs)

Test Specimen	Projected Area A (ft ²)	Relative Velocity U (ft/s)	Drag Coefficient (C _d)	
			0.6	1.0
Small PCI Prototype No. Test-1	5.28 (6.48)	2	12	20
		4	49	82
		6	110	184
		8	196	327
		10	307	511
Large PCI Strainer Prototype No. 2	12.0 (14.3)	2	28	46
		4	112	186
		6	251	418
		8	446	744
		10	697	1162
Reference Cylinder 30" φ x 33 1/4"	6.93	2	16	27
		4	64	107
		6	145	241
		8	258	429
		10	402	671

Note: Projected area is net frontal area projected normal to flow direction. Gross envelope projected areas for the stacked disk strainers (including area of disk slots) are shown in parentheses.

TABLE 4.7

CALCULATED INERTIA FORCES (lbs)

Test Specimen	Weight W (lbs)	Mass Coefficient C_m	Displaced Water Weight $\rho g V$ (lbs)	Total Weight $W + C_m \rho g V$ (lbs)	Acceleration dU/dt (ft/s ²)	
					1.5	3.0
Small PCI Prototype No. Test-1	305	1.0	564	869	40.5	81.0
		1.5	846	1151	53.6	107
		2.0	1128	1433	66.8	134
Large PCI Strainer Prototype No. 2	948	1.0	1638	2586	121	241
		1.5	2457	3405	159	318
		2.0	3276	4224	197	394
Reference Cylinder 30" ϕ x 33 1/4"	324	1.0	842	1166	54.3	109
		1.5	1263	1587	73.9	148
		2.0	1684	2008	93.5	187

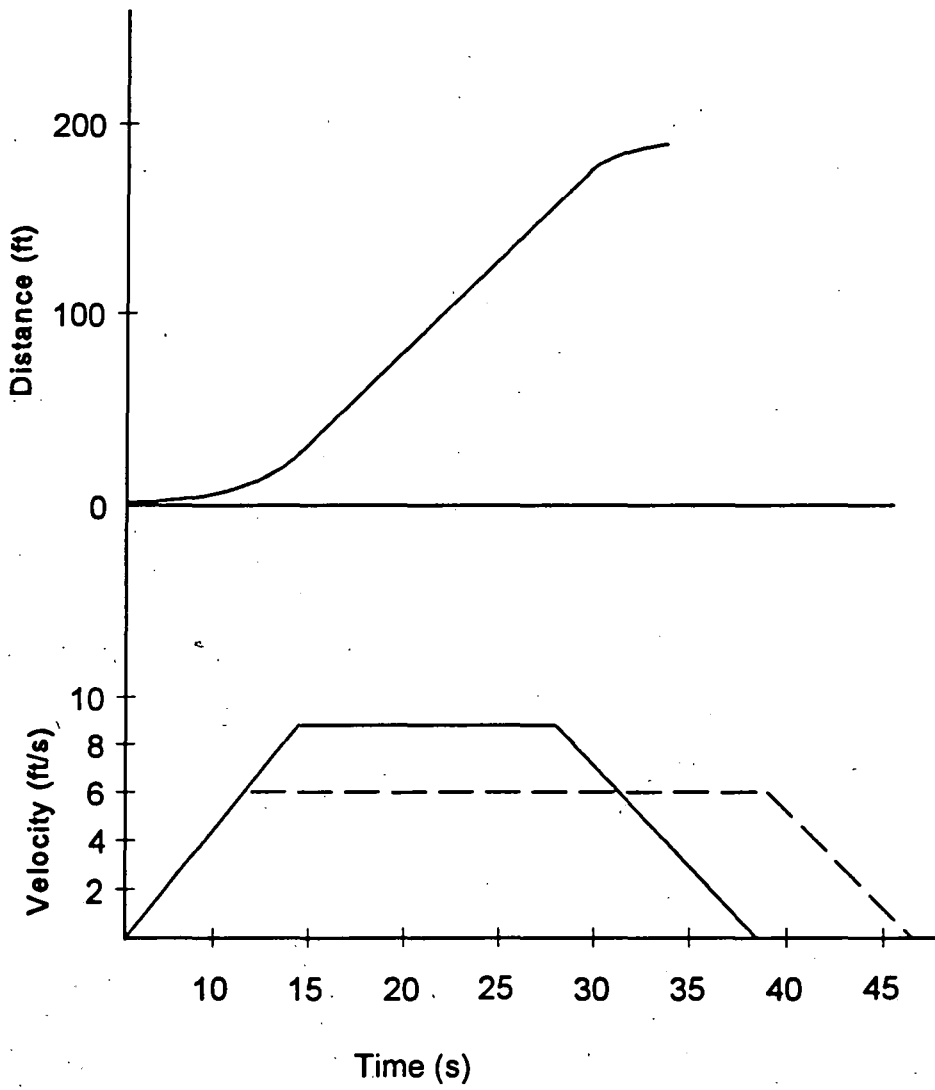


FIGURE 4.1

EXAMPLE OF TARGET TRAVEL DEFINITION

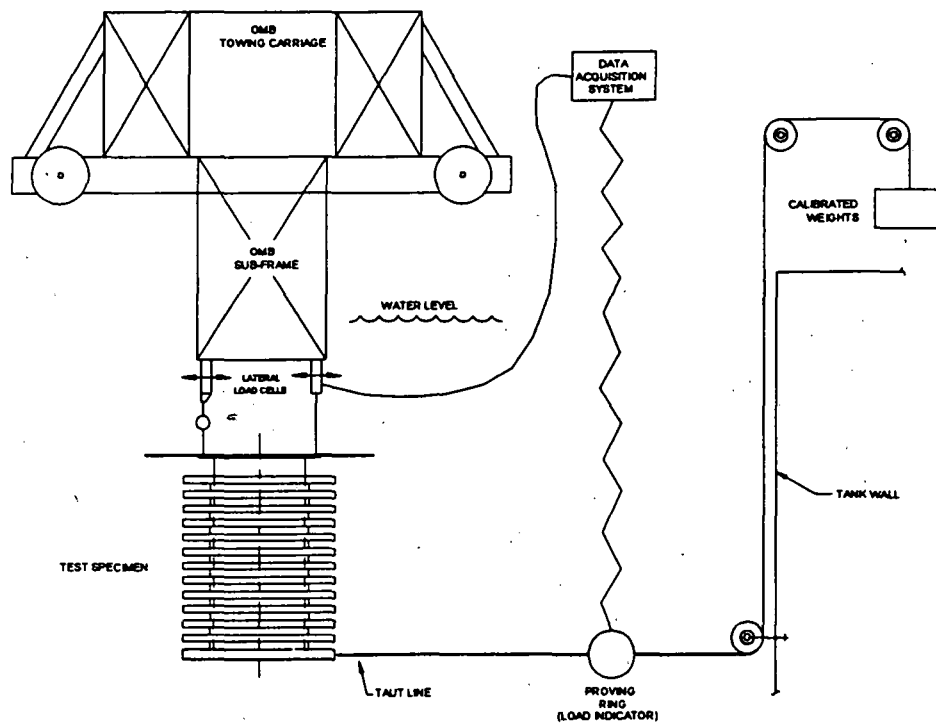


FIGURE 4.2

LAYOUT OF LOAD CALIBRATION SYSTEM

5.0 RESULTS

5.1 Approach to Results Interpretation

Consistent with the basic approach to empirical hydrodynamics as applied in the structural qualification of submerged structures in BWR suppression pools, the empirically-based Morison equation for separated flow around cylinders was the basis for interpretation of the test results. Even though the Morison formulation is empirical, there are several theoretical considerations that will lead to the same form as the Morison equation and to numerical values of a dimensionless force coefficient. The inertia, or mass term in the equation is identical with the linear force term derived by potential flow theory, which forms the basis for submerged structure loads in BWR suppression pools.

The Morison approach considers the hydrodynamic force, F_h , to consist of a drag component, F_d , and an inertial component, F_m . The drag component is proportional to the square of the free-stream fluid velocity, U , (relative to a fixed cylinder) whereas the inertial component is proportional to the free-stream fluid acceleration, dU/dt . The relationship is expressed as follows:

$$F_h = F_d + F_m \quad \text{Eq [3]}$$

where,

$$F_d = \frac{1}{2} C_d \rho A U|U|$$

and

$$F_m = C_m \rho V dU/dt$$

Changing the frame of reference, the same force components exist when the cylinder is accelerated through still water (i.e. the relative motion between the fluid and cylinder are maintained). The large basin (width, length and depth) ensures that edge effects are minimized so that the towing velocity is a good representation of free-stream velocity.

By measurement of the total forces to accelerate the submerged test specimen through the basin, and a separate measurement of the drag forces and submerged

body acceleration, the hydrodynamic inertial forces can be derived, from which an effective mass coefficient, C_m , was determined. The towing test results are analyzed and discussed under the separate sections of constant velocity (zero acceleration) and accelerated motion.

5.2 Constant Velocity Towing (Drag Forces)

The initial tests in each series were used to obtain the drag characteristics of each test specimen. Once the target terminal velocity for a test was attained, the towing continued at a relatively constant free-stream velocity enabling the drag force to be calculated. During this stage, the free-stream acceleration was effectively zero and the inertial forces were accordingly zero so that the total force can be attributed to drag.

For the towing tests with the high terminal velocities (10 ft/s) and the low acceleration (0.5 ft/s^2), the duration of constant velocity is zero (for example, see Figure 5.1, a velocity plot of Test d105a). The constant velocity sections of the high acceleration towing tests were used to obtain drag at high velocities.

The history of total drag for each test was obtained by summing the three measured lateral loads, FX1, FX2 and FX3. A typical history of the resulting drag, X-Force, for Test d104 is shown in Figure 5.2. The associated velocity history is plotted in Figure 5.3.

The tare drag loads generated by the mounting assembly were calculated from the appropriate constant-velocity section of the 200 Series (support and boundary assembly tested by towing alone) as shown for Test d203 in Figure 5.4. These tare drags were subtracted from the drag loads derived from the other towing tests to obtain the net drag forces, F_d , which are given in Tables 5.1 and 5.2.

The drag load was related to the net projected (frontal) area, A , and nominal velocity, U , to obtain a drag coefficient, C_d . These calculated C_d values are also shown in Tables 5.1 and 5.2.

The complete drag results for the two strainers are presented in Table 5.1.

< Proprietary Information Removed >

The drag results for the reference smooth bodies are presented in Table 5.2.

< Proprietary Information Removed >

A plot of the history of derived overturning moment (with respect to the flange elevation) for Test d187 is shown in Figure 5.5. The resulting lever arm (effective point of application of the total hydrodynamic force) was obtained by dividing the overturning moment by the total force and is plotted for the duration of Test d187 in Figure 5.6. For the test duration (approximately 4.7 to 23.3 seconds) the consistent effective point of load application (height of 1 ft below flange) is apparent. After correcting for the adapter assembly loads, this point is approximately at the center of gravity of the strainer.

5.3 Accelerated Towing (Hydrodynamic Mass)

The hydrodynamic mass of the test specimens was investigated by examining the initial impulse phase of the higher acceleration towing tests. At the lower accelerations, the inertial forces are not sufficient to provide robust estimates.

The benefit of using the initial impulse is that the initial flow conditions are truly static (zero velocity and acceleration) and specimen velocities do not attain any significant value for the duration of the initial impulse (application of the target carriage acceleration). Thus the incremental horizontal force applied to the test specimen is solely the inertial force due to the incremental acceleration from rest to some small period of time after motion initiation.

Results from investigation of the initial impulses for the strainers are presented in Table 5.3. The initial impulse (differential acceleration from rest to first reversal) is listed together with the corresponding impulsive force. The inertial mass (total for the test system below the load cells), W/g , was obtained from application of basic dynamics (Newton's Second Law, $F=m \cdot dU/dt$). Note that the masses are expressed as weights, mass $\cdot g$, in the table.

< Proprietary Information Removed >

The coefficient of hydrodynamic mass was subsequently derived from the following:

$$C_m = (W_i - W_s - W) / \rho g V \quad \text{Eq [4]}$$

The calculated hydrodynamic mass coefficients for the large strainer, based on enclosed displaced volume, range from < Proprietary Information Removed >. These results are not unexpected as discussed below.

Results for the small strainer indicate < Proprietary Information Removed >

A sample result for the reference smooth impervious strainer body is provided in Table 5.4 and indicates < Proprietary Information Removed >. As discussed below, the existence of vortex shedding tended to complicate response for the smooth stacked disk and thus the results proved to be unreliable.

5.4 Free Vibrations

The free-vibration response of the quick-release tests on each of the test specimens in the carriage-mounted submerged condition was analyzed to determine:

- a. Test specimen natural oscillation frequencies
- b. Test specimen free-vibration damping

The dominant oscillation frequencies were obtained by simple measurements from the oscillation history plots. Damping factors, C/C_{cr} , (fraction of critical) were obtained from calculations of the logarithmic decrement, δ , typically using three or four cycles of response:

$$\delta = \ln(X_{n+1}/X_n) = 2\pi(C/C_{cr})(w/w_d) \quad (\text{Reference 5.1}) \quad \text{Eq [5]}$$

Typical acceleration history records for the duration of free oscillation for both the small and large test strainers are shown in Figures 5.7 and 5.8. The associated load history in one of the horizontal load cells is shown in Figure 5.9 which indicates the initial offset due to applied load.

Results for the four test specimens are summarized in Table 5.5.

< Proprietary Information Removed >

< Proprietary Information Removed >

TABLE 5.1

CONSTANT VELOCITY TOWING TEST RESULTS
STRAINER DRAG FORCES

Test Number	Projected Area A (ft ²)	Nominal Velocity U (ft/s)	Total Drag F (lbs)	Support Drag F _s (lbs)	Net Drag F _d (lbs)	F _d /U ²	Calculated Drag Coefficient (C _d =2F _d /ρAU ²)
d101							
d102							
d103	5.28						
d103a							
d104	Prototype						
d104a	No. Test-1						
d105	(Small)						
d105a							
d501a							
d502							
d503	12.0						
d504							
d505	Prototype						
d562	No. 2						
d572	(Large)						
d582							
d505a							

< Proprietary Information Removed >

TABLE 5.2

CONSTANT VELOCITY TOWING TEST RESULTS
REFERENCE BODY DRAG FORCES

Test Number	Projected Area A (ft ²)	Nominal Velocity U (ft/s)	Total Drag F (lbs)	Support Drag F _s (lbs)	Net Drag F _d (lbs)	F _d /U ²	Calculated Drag Coefficient (C _d =2F _d /ρAU ²)
d301							
d302							
d303	6.92						
d386							
d304	Smooth						
d362	Cylinder						
d305							
d401							
d402							
d403	5.28						
d404							
d405	Smooth						
d452	Impervious						
d462	Strainer						

< Proprietary Information Removed >

TABLE 5.3

INITIAL IMPULSE TOWING TEST RESULTS
STRAINER INERTIA FORCES

Test Number	Test Specimen Weight (lbs)	Impulse Acceleration dU/dt (ft/s ²)	Impulse Force F_i (lbs)	Inertial Weight W_i (lbs)	Support Weight W_s (lbs)	Net Weight $W_i - W_s$ (lbs)	Mass Coefficient $C_m = (W_i - W_s - W)/\rho g V$
d187							
d186	Prototype						
d185	No. Test 1						
d182							
d171	W=305						
d162	$\rho g v = 564$						
d161							
< Proprietary Information Removed >							
d582	Prototype						
d572	No. 2						
d562	W=948						
d552	$\rho g v = 1638$						

TABLE 5.4

INITIAL IMPULSE TOWING TEST RESULTS
REFERENCE SMOOTH CYLINDER INERTIA FORCES

Test Number	Test Specimen Weight (lbs)	Impulse Acceleration dU/dt (ft/s ²)	Impulse Force F _i (lbs)	Inertial Weight W _i (lbs)	Support Weight W _s (lbs)	Net Weight W _i - W _s (lbs)	Mass Coefficient C _m = (W _i - W _s - W) / ρgV
d386	W=324 ρgv=842		< Proprietary Information Removed >				

TABLE 5.5

FREE VIBRATION TEST RESULTS

Test Number	Test Specimen	Frequency (Hz)	Critical Damping Ratio
d198 d198a d198b	Prototype No. Test-1		< Proprietary Information Removed >
d398 d398a d398b	Smooth Cylinder		
d498 d498a d498b	Smooth Impervious Strainer		
d598 d598a d598b d598c	Prototype No. 2		

< Proprietary Information Removed >

FIGURE 5.1

VELOCITY HISTORY - TEST d105a

< Proprietary Information Removed >

FIGURE 5.2

PROTOTYPE NO. TEST-1 DRAG FORCE HISTORY - TEST d104

< Proprietary Information Removed >

FIGURE 5.3

PROTOTYPE NO. TEST-1 VELOCITY HISTORY - TEST d104

< Proprietary Information Removed >

FIGURE 5.4

SUPPORT DRAG FORCE HISTORY - TEST d203

< Proprietary Information Removed >

FIGURE 5.5

PROTOTYPE NO. TEST-1
DERIVED OVERTURNING MOMENT HISTORY - TEST d187

< Proprietary Information Removed >

FIGURE 5.6

PROTOTYPE NO. TEST-1 EFFECTIVE LEVER ARM - TEST d187

< Proprietary Information Removed >

FIGURE 5.7

PROTOTYPE NO. TEST-1 FREE VIBRATION ACCELERATION - TEST d198a

< Proprietary Information Removed >

FIGURE 5.8

PROTOTYPE NO. 2 FREE VIBRATION ACCELERATION - TEST d598

< Proprietary Information Removed >

FIGURE 5.9

PROTOTYPE NO. 2 FREE VIBRATION LOAD CELL FZ1 FORCE - TEST d598

6.0 DISCUSSION OF RESULTS

6.1 Approach to Results Interpretation

The original intention of using the accelerated flow regime of the tests at the higher accelerations to terminal velocity to obtain the effective inertial mass of each test specimen was not followed. Essentially, there were large variations from a constant value in the test specimen acceleration, due principally to carriage acceleration control through the servo-system and local vibration modes of the carriage structure. This variation made separation of drag and inertia forces difficult and thus use of initial impulse information became the preferable approach.

6.2 Coefficients of Drag

The range of derived drag coefficients, C_d , for the smooth cylinder < Proprietary Information Removed > is reasonable when compared with classical empirical data as illustrated in Figure 6.1. Reynolds numbers for the cylinder towing tests were within the range

< Proprietary Information Removed >.

As expected, the drag coefficients for the perforated strainers, < Proprietary Information Removed >, are much higher than those for the enveloping smooth cylinder and the artificially non-perforated stacked disk. The perforations were anticipated to increase drag resistance (due to roughness). The gross surface area (porous) of the stacked disk is 2.49 times that of the reference cylinder and the higher drag for the former was expected. The net surface area (excluding holes) for the perforated plate with 40 percent holes is 1.49 ($=2.49 \cdot 0.6$) times that of the reference cylinder.

6.3 Coefficients of Hydrodynamic Mass

The standard inertial mass coefficient of 2.0 for a cylinder refers to the two-dimensional body i.e., an infinitely long cylinder. Three-dimensional correction to C_m , per accepted ABS rules (Reference 6.1), for the reference cylinder would suggest a correction factor, K , of 0.83 considering the flanged-end boundary as infinite (length to diameter ratio, $l/d = 33.25/30. = 1.108$ with one free end, so that the effective l/d is 2.217).

Due to the strainer spool (reduced diameter of flanged-end boundary), the three-dimensional correction for the stacked disk strainers, assuming cylindrical

behavior, would be expected to lie between the values derived assuming no boundary effects at either end and a full boundary at the flange end. For the small strainer (assuming a cylinder based on the disk diameter) the resulting correction factor ranges from 0.55 to 0.83, and for the large strainer, from 0.65 to 0.88. Thus significant reductions in the inertial mass coefficient are expected due to the three-dimensional end effect alone. < Proprietary Information Removed >.

Additional reduction due to perforations is expected. Although perforations increase drag, they reduce hydrodynamic inertia by allowing flow through a perforated body. They also reduce vortex shedding.

The three-dimensional end effect is expected to be less for the perforated strainer than for the impervious smooth cylinder due to the relatively less restricted flow afforded the perforated body (which is reason for the lower inertial hydrodynamic mass coefficient in the first place i.e., less contained and entrained fluid).

6.4 Vortex Shedding

< Proprietary Information Removed >

6.5 Free Vibrations

Comparison of the results for the small strainer tests alone, as a uniform smooth non-perforated test cylinder, and as a smooth impervious non-perforated stacked disk body indicate the change in free oscillation frequency which is indicative of the inertial mass of the test specimen. Of significance, the considerably higher frequency of the small strainer compared to the non-perforated cylinder and stacked-disk body indicates the distinctly lower effective inertial mass of the perforated strainer.

Given that the stiffness of the supported system is effectively the same for each specimen, the ratio of frequencies is inversely proportional to the effective mass of the system.

< Proprietary Information Removed >

These results strongly support the lower hydrodynamic mass coefficient values for the perforated bodies when compared with traditional smooth impervious cylinders.

6.6 Perforations and Hydrodynamic Mass Coefficients

The hydrodynamic mass for the analyses of submerged structures in ECCS suppression pool applications is typically based on an inertial mass coefficient, C_m ,

of 2.0, defined such that the added mass coefficient is 1.0. With this definition, the C_m value for a flooded impervious body is always greater than one. For a perforated body the "contained" mass has no lower limit; the fluid may be able to flow in and out at will if the perforated body is sufficiently "open". < Proprietary Information Removed > .

From another perspective, the hydrodynamic mass may be viewed as the manifestation of pressure differentials due to the flow field. The perforations effectively negate or "relieve" the pressure. The degree of "openness" required to allow this pressure relief has not been determined here but is judged to be small.

6.7 Application of Test Results

A number of factors, principally geometric, are likely to affect the hydrodynamic parameters derived from these tests. These geometric factors are shown in Table 6.1 and include:

< Proprietary Information Removed >

The hydrodynamic parameters derived from the test results of this investigation are applicable to stacked disk strainers similar with respect to the above geometric parameters to those tested.

TABLE 6.1

GEOMETRIC PARAMETERS OF TESTED STRAINERS

Parameter	Prototype No. Test-1	Prototype No. 2
Strainer Length to Diameter Ratio	1.00	1.20
Disk to Slot Thickness Ratio	1.66	0.90
Spool Length to Diameter Ratio	0.31	0.23
Strainer Hole to Surface Area	40%	40%
Strainer Hole Diameter	1/8"	1/8"

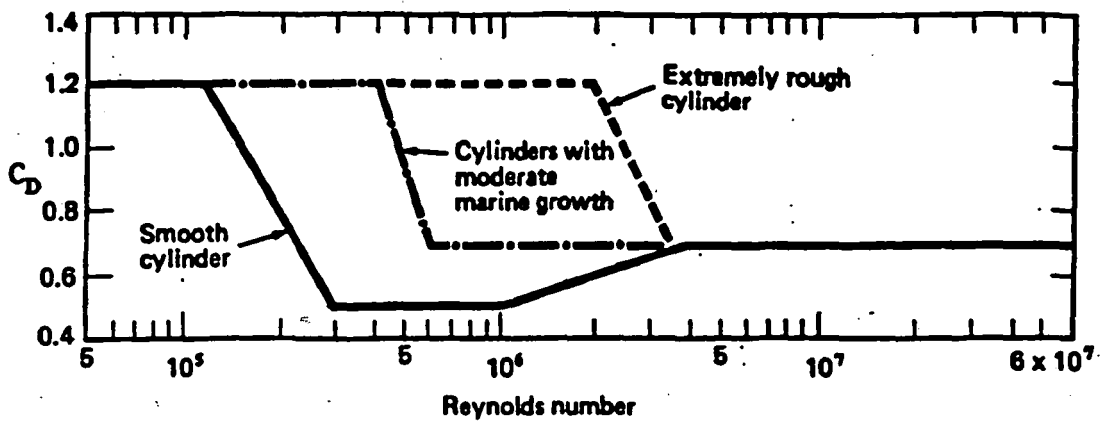


FIGURE 6.1

RECOMMENDED DRAG COEFFICIENT VALUES
(Reference 6.2)

< Proprietary Information Removed >

FIGURE 6.2

SMOOTH IMPERVIOUS STRAINER DRAG FORCE - TEST d472

7.0 CONCLUSIONS

A test program was conducted to investigate the behavior of large capacity stacked disk ECCS suction strainers subjected to accelerated separated fluid flow fields. Empirically based values for the coefficients of constant velocity drag, C_d , and hydrodynamic (inertial) mass, C_m were obtained by accelerating the test objects through still water and by submerged free vibration tests. The tests were performed using PCI Sure-Flow™ stacked disk strainer prototypes No. Test-1 and No. 2

The significant conclusions drawn from the reduction of the data recorded during the tests are as follows:

- The hydrodynamic coefficient of drag C_d , as expected, is higher than that for an impervious smooth cylindrical body of same major dimensions.

< Proprietary Information Removed >

- The resultant coefficient of inertial mass, C_m , is substantially lower than that for an impervious smooth cylindrical body of same major dimensions.

< Proprietary Information Removed >

These conclusions are applicable in the lateral direction to stacked disk strainers which are similar to the PCI prototype designs tested. Section 6 of this report discusses in detail those parameters which significantly influence the conclusions and which must be evaluated to determine their applicability for strainers of different geometric proportions.

8.0 REFERENCES

- 1.1 NRC Bulletin 96-03, "Potential Plugging of Emergency Core Cooling Suction Strainers by Debris in Boiling-Water Reactors," May 6, 1996
- 1.2 Morison, J.R., O'Brien, M.P., Johnson, J.W., and Schaaf, S.A., "The Force Exerted by Surface Waves on Piles," Petroleum Transactions, AIME, Vol. 189, pp. 149-154, 1950
- 2.1 Performance Contracting, Inc., Engineered Systems Division, Kansas, BWR Test Strainer, Drawing Numbers: ECCS-1, ECCS-2, Rev 0, 02-10-93
- 2.2 Performance Contracting, Inc., Engineered Systems Division, Kansas, ECCS Suction Strainer, Drawing Number: ECCS-003, Rev 1, 07-31-95
- 3.1 Duke Engineering & Services, Inc., Specification No.: TS-ECCS-QC-01, "Hydrodynamic Mass Determination for PCI Sure Flow ECCS Suction Strainer", Report No. VQ16RD.F13, Rev. 0, November, 1996
- 3.2 386-MATLAB for 80386-based MS-DOS Personal Computer, October 15, 1990
- 5.1 John M. Biggs, "Introduction to Structural Dynamics," McGraw-Hill, Inc. 1964
- 6.1 American Bureau of Shipping, "Rules for Building and Classing Mobile Offshore Drilling Units," 1980 Edition
- 6.2 Atkins Research and Development; CIRIA Underwater Engineering Group, "Dynamics of Marine Structures - Methods of Calculating the Dynamic Response of Fixed Structures Subject to Wave and Current Action," Report UR8, June 1977.

APPENDIX A

LIST OF TEST INSTRUMENTATION

LIST OF TEST INSTRUMENTATION

1. Load Cell Strain Gages

Precision Strain Gages, Micro-Measurements Inc.
CEA Stacked Rosette Model, Type CEA-13-062WT-350

2. Load Indicators

Bending Beam Load Cell, Transducers Inc.
Model T363-1K-20P1, S/N 06012

Weighing Indicator, A&D Co. Ltd, Tokyo
Model AD-4316, Option List 01020304, S/N B 0800812

3. Accelerometer

Q-Flex Servo Accelerometer, Sundstrand Data Control, Inc.
Model QA-700, P/N 979-0700-001, S/N 7948

4. Angle Measurer

Angle Computer Co., Inc.
S/N C274

5. Tachometer

OMB Towing Carriage Tachometer
PMI Model 12FS 089

APPENDIX B
CALIBRATION DATA

B-1. Load Calibration

All weights used for load Calibration and calibration checks were verified as being within the maintenance tolerances applicable to scales according the appropriate California Code of Regulations. This tolerance is 0.1% of the test load. All test weights were certified traceable to NIST as documented herein.

The Reference Load Indicator was directly checked against the certified weights.

< Section B-1 information is proprietary in its entirety >

B-2. Calibration Data

The plots in this Section represent the calibration data for the load cells used in the tests. All loads are referenced to the Reference Load Indicator which was calibrated using weights traceable to the NIST, as discussed in Section B-1.

< Section B-2 information is proprietary in its entirety >

B-3. Velocity and Acceleration Calibration Data

The OMB towing carriage tachometer was calibrated against the certified hand-held tachometer and also against direct distance and time measurements. (Time to travel 50 ft at preset terminal velocity measured with stop watch - variation less than 0.5%)

< Section B-3 information is proprietary in its entirety >